

NACA RM E56K27a

62 64164

214

Copy
RM E56K27a

NACA

GPO PRICE \$

OTS PRICE(S) \$

Hard copy (HC) 2.00

Microfiche (MF) .50

V-1338

RESEARCH MEMORANDUM

BRIEF STUDIES OF TURBOJET COMBUSTOR AND FUEL SYSTEM

OPERATION WITH HYDROGEN FUEL AT -400° F

By David M. Straight, Arthur L. Smith, and Harold H. Christenson

Lewis Flight Propulsion Laboratory
Cleveland, Ohio

DECLASSIFIED - EFFECTIVE 1-15-64
Authority: Memo Geo, Drobka NASA HQ
Case ATSS-A Dtd. 3-12-64 Subj: Change
in Security Classification Marking

N65-12708

ACCESSION NUMBER

(THRU)

(CODE)

33

(CATEGORY)

(PAGES)

(NASA CR OR TM OR AD NUMBER)

NATIONAL ADVISORY COMMITTEE
FOR AERONAUTICS

WASHINGTON

March 7, 1957

Reclassified May 29, 1959

FORM 608

NATIONAL ADVISORY COMMITTEE FOR AERONAUTICS

RESEARCH MEMORANDUM

BRIEF STUDIES OF TURBOJET COMBUSTOR AND FUEL-SYSTEM

OPERATION WITH HYDROGEN FUEL AT -400° F *

By David M. Straight, Arthur L. Smith, and Harold H. Christenson

SUMMARY

A single J33 combustor and an experimental tubular combustor incorporating a fuel vaporizer were operated with gaseous hydrogen at temperatures slightly above the boiling point of the fuel. Data were obtained to explore possible effects of the fuel temperature on combustor performance and on the control and measurement of fuel flow. Combustion efficiencies and combustor outlet temperature profiles were determined over a range of combustor inlet-air pressures from 4 to 40 inches of mercury absolute and at a combustor inlet-air temperature of 300° F. For comparison, similar data were obtained with hydrogen fuel at ambient temperatures.

In general, combustion efficiency was near 100 percent for both combustors and for both the cold and the warm fuels. Combustor outlet temperature profiles were similar to those obtained with liquid hydrocarbon fuels in the J33 combustor and were not affected by the temperature of the fuel. The vaporizing combustor produced an outlet temperature profile having a hot core.

Measurements of the transfer of heat to the boiling liquid hydrogen in the 3/4-inch vacuum-insulated transfer piping indicated a heat-leak rate of approximately 38 Btu per hour per foot of length. Pressure and temperature oscillations were observed in portions of the system where boiling of the fuel occurred; however, it is believed that these oscillations can be eliminated by further refinement in the fuel system.

In addition to the combustor tests, a finned-tube heat exchanger, such as may be used to vaporize liquid hydrogen, was subjected to large temperature transients by introducing cold fuel at fuel temperatures near -400° F while the heat exchanger was immersed in a 1500° F gas stream. No noticeable damage occurred after several trials.

*Title, Unclassified.

DECLASSIFIED - EFFECTIVE 1-15-64
 Authority: Memo Geo. Drobka NASA HQ.
 Code ATSS-A Dtd. 3-12-64 Subj: Chang
 in Security Classification Marking

12708 . 0

[Handwritten signature]

INTRODUCTION

Considerable improvements in aircraft range and altitude may be realized with the use of liquid hydrogen as a fuel (ref. 1). In addition, substantial gains in turbojet combustor performance can be obtained with the use of warm gaseous hydrogen (refs. 2 and 3). Further, reference 4 shows that, with the use of gaseous hydrogen, combustor length can be reduced without sacrificing combustor performance. The practical use of hydrogen for turbojet engines requires that it be stored as a liquid in the fuel supply tanks. Ultimately, the large heat sink available in the cold liquid fuel would be used to cool various parts of the airplane and the engine, and warm gaseous fuel would then be supplied to the combustor. However, in the early development phases of hydrogen-fueled aircraft, fuel systems and combustion chambers may have to operate with cold gaseous hydrogen at temperatures slightly above its boiling point. Also, during takeoff and low-speed flight of a hydrogen-fueled aircraft, cooling requirements would be greatly reduced, and fuel temperatures slightly above the boiling point may be encountered at the combustor. The investigation reported herein was conducted to determine whether there is any adverse effect of cold fuel on combustor performance and to gain operating experience in the measurement and control of fuel flow at these low temperatures.

Two different combustor designs were operated with cold gaseous hydrogen fuel. The first design, a J33 combustor with a modified fuel nozzle, was operated over a range of combustor inlet-air pressures from 4 to 30 inches of mercury absolute. The second combustor design incorporated vaporizing tubes in which the fuel mixed with some of the air before it entered the combustion zone. This combustor was operated at inlet-air pressures of 36.6 and 40.6 inches of mercury absolute. The performance data obtained with these combustors include combustion efficiency and the temperature profile at the combustor outlet.

Descriptions of the special equipment, instrumentation, and operating techniques required for the control and measurement of liquid and gaseous hydrogen flows at temperatures close to the boiling point are included herein. The liquid hydrogen was supplied under pressure from a storage Dewar tank. Two types of heat exchanger were used to vaporize the fuel before it entered the combustor. For the J33 combustor tests, a concentric-tube heat exchanger was used in which helium was used as a source of heat. For some of the runs with the vaporizer-tube combustor, a finned-tube heat exchanger was installed in the exhaust section downstream of the combustor.

REF ID: A66015

APPARATUS AND PROCEDURE

Combustors

Installation. - The test combustors were installed in a connected-duct facility as shown in figure 1. Combustion air from the laboratory supply system flowed first through a sharp-edged orifice for measuring the airflow rate and then through an electric heater for controlling the combustor inlet-air temperature. The airflow and pressure at the combustor test section were controlled by regulating valves in the air supply line and in the altitude exhaust system. Water sprays located in the exhaust section cooled the exhaust gases and diluted them with water vapor to reduce the over-all mixture ratio to a safe level in the event some of the fuel did not burn in the combustor.

J33 Combustor. - A J33 combustor with a modified fuel nozzle (fig. 2) was chosen for this investigation, since reference performance data with warm fuel were available (ref. 2). Hydrogen was injected through six 0.063-inch holes equally spaced about the axis of the nozzle tip and inclined at an angle of 45° from the axis (fig. 2). In addition, one hole 0.016 inch in diameter injected fuel along the axis. Ignition was provided by a standard ignitor located in the dome area of the combustor liner. The combustor was operated at inlet-air pressures of 4, 8, 15, and 30 inches of mercury absolute with cold fuel, and at 4, 8, and 15 inches of mercury absolute with hydrogen fuel at ambient temperatures.

Vaporizer-tube combustor. - The vaporizing-tube combustor was designed to simulate the combustion process that occurs in several current full-scale engines. A photograph of the combustor is shown in figure 3. The proportioning of the entrance air-hole areas in the liner was patterned after a current vaporizer-tube combustor. The dummy liquid-fuel injectors shown in figure 3 were installed to simulate the added blockage of the vaporizer-tube area that would exist if hydrocarbon feed tubes were installed for alternate fuel operation. Ignition was provided by a spark gap formed between a wire connected to a high-voltage transformer and a metal surface in the dome region of the combustor liner. The vaporizing-tube combustor was operated at the following inlet-air conditions: pressure of 36.6 and 40.6 inches of mercury absolute, reference velocity of about 65 feet per second, and temperature of 300° F. In addition, the combustor was operated at a high reference velocity (191 ft/sec) to simulate the conditions in an engine tailpipe (670 ft/sec in combustor outlet section) for the tailpipe heat-exchanger tests.

Instrumentation. - Instrumentation stations are shown in figures 1 and 2. Total-pressure tubes were manifolded together at stations A and D, and the average reading of each station was indicated on absolute manometers. Average and individual thermocouple readings from stations B and C were indicated on self-balancing potentiometers. Construction

details of the total-pressure tubes and of the thermocouples used are shown in figure 4. The Chromel-Alumel thermocouples for measuring combustor outlet temperatures (station C) were of the bare-wire crossflow type with a large length-to-diameter ratio to minimize conduction errors (ref. 5).

An attempt was made to verify the combustion-efficiency values calculated from the outlet thermocouple measurements by using gas analysis. Six of the outlet total-pressure tubes were used to obtain a sample of the exhaust gases. The sample was passed through dryers to remove the water vapor and then analyzed by a thermal-conductivity method. Since hydrogen has approximately seven times the thermal conductivity of the other constituents of the mixture, a high degree of sensitivity was achieved. However, the sampling tubes were not cooled, and unburned fuel present in the exhaust products may have reacted in the sampling tubes because of catalytic action of the hot metal surfaces of the sampling tubes.

Fuel System

A schematic diagram of the fuel system is presented in figure 5, showing the basic piping, valves, instrumentation, and so forth, for control and measurement of the fuel flow. Liquid hydrogen was stored under pressure of hydrogen gas in the Dewar. During operation, the liquid fuel flowed through vacuum-insulated transfer piping to the heat exchanger, where it was vaporized. The cold gas flowed through an emergency remotely operated fuel shutoff valve (J), a throttle valve (K), and an orifice (M) to the combustor. The vacuum-insulated piping extended from the Dewar to the inlet of the orifice run; from this station to the combustor connection, a synthetic foamed plastic was used for insulation. The other piping shown in figure 5 was necessary for pressurizing the Dewar, purging the system, flowing helium to the heat exchanger, and relieving excessive pressures in the system through relief valves. Before operation, the system was checked for leaks with soap suds when the system was warm, or with a gas analyzer when the system was cold.

To start operation, the system was first evacuated with the vacuum pump. The system was then filled with helium under pressure, re-evacuated, and filled again with helium to assure that no air was left in the system. Some helium was allowed to flow into the combustor to purge the nozzle feed line. Before cold fuel was fed into the system, the heat-exchanger helium flow was turned on to prevent air from condensing in the heat exchanger. After the ignition spark was turned on, the cold fuel was admitted to the system. The fuel temperature at the combustor was controlled by varying the helium flow through the heat exchanger or by turning off the helium and evacuating the heat-exchanger outer shell with the vacuum pump.

DECLASSIFIED

Dewar. - A schematic diagram of the Dewar supply tank is shown in figure 6. The Dewar consisted of an inner tank (a) containing the liquid hydrogen, surrounded, in turn, by an evacuated chamber (b), a liquid-nitrogen tank (c), and a second evacuated chamber (d). The liquid nitrogen reduced the heat-leak rate due to radiation from the outer shell to the inner tank, and the vacuum chambers reduced the heat leak due to convection and conduction.

Some of the associated measuring and control equipment are also shown in figure 6. Provision was made for filling and draining both the nitrogen and hydrogen tanks and for venting the gases boiled off from the liquid. Pressure in both tanks was controlled by manual and automatic pressure-relief valves.

Piping and valves. - The construction of the vacuum-insulated fuel line is shown in figure 7. The fuel line consisted of a 3/4-inch stainless-steel pipe wrapped with aluminum foil, spaced inside a 1.5-inch copper shell. The space between the two pipes was sealed and evacuated to a pressure of about 3 microns of mercury absolute. A bellows was spliced into the inner tube to relieve stresses in the pipes due to thermal expansion. A carbon-block gas absorber was installed about every 2 feet along the length of the tubes to absorb residual gases in the annulus. The sections of vacuum-jacketed tubing were connected by special unions that provided for an overlap of the vacuum jacket to reduce the heat leak.

Construction of a typical valve for cold-flow service is also shown in figure 7. The valve stem and the bonnet were extended about 12 inches from the valve seat. Both the valve stem and the bonnet were vacuum-insulated; thus, the valve seal and the threads were in a warmer location to assure proper valve operation. For remotely operated valves, the valve stem was actuated by a pressure-operated piston.

The entire transfer system contained a number of components representative of a typical fuel system. The over-all length of piping was about 22 feet and contained the following components: two T's, two valves, five 90° bends, 4 feet of straight pipe, and a short flexible connection. These components were connected by 11 unions.

Heat exchangers. - The counterflow concentric-tube heat exchanger used to vaporize the liquid hydrogen fuel was provided by modifying an 8-foot-long section of the vacuum-insulated transfer pipe. A short piece of 3/4-inch copper tubing was soldered to the outer shell of the transfer pipe at each end to provide inlet and outlet connections for helium. Installation of the tailpipe heat exchanger in the combustor exhaust duct is shown in figure 8(a). The control valves in the fuel line for directing the fuel flow through the heat exchanger or through a bypass line are also shown. Figure 8(b) is a photograph of the heat

exchanger. Thin, closely packed (approximately 32 per in.), spiral fins were attached to a 0.375-inch-diameter, 0.03125-inch-wall stainless-steel tube. The fins were copper covered with stainless steel. Tests of instantaneous introduction of cold fuel on the hot inner surface of the heat exchanger were conducted by first flowing fuel through the bypass into the combustor. Combustor outlet temperature and velocity of approximately 1500° F and 670 feet per second, respectively, were established to simulate engine tailpipe conditions. After the heat-exchanger metal temperatures were stabilized at some temperature near the gas temperature, the fast-acting valves were switched and the cold gaseous hydrogen at approximately -400° F flowed through the heat exchanger. No interruption in combustion was noted during the transition.

Fuel-system instrumentation. - The temperature of the fuel was measured with copper-constantan thermocouples at the inlet and outlet of the concentric-tube and tailpipe heat exchangers and at the orifice (figs. 5 and 8(a)). Construction details of thermocouples installed at the inlet and outlet of the orifice run are shown in figure 9. The thermocouples at the inlet of the orifice run and one of two thermocouples at the outlet were shielded to reduce radiation from the walls of the orifice run. The second outlet thermocouple was a bare-wire crossflow type. Thermocouple connector plugs were mounted above the level of the orifice run to prevent the liquid air that formed on the piping from reaching the plug.

Construction details of the orifice used for measuring fuel-flow rates are also shown in figure 9. The inlet pressure and the pressure drop across the orifice were measured with 100-inch mercury manometers; for low flow rates a 100-inch water manometer was used. The helium flow through the outer shell of the heat exchanger was measured with a sharp-edged orifice instrumented with a pressure gage, and a differential pressure manometer. The temperature of the helium entering and leaving the heat exchanger was also measured.

Calculations and Calibrations

Combustor performance. - Combustion efficiency was calculated as the percentage ratio of actual to theoretical increase in enthalpy from the combustor inlet to the combustor outlet instrumentation plane (ref. 2). The calculation of fuel-flow rate, the calibration of the fuel temperature thermocouples, and the corrections applied to the combustor exhaust-gas temperature indications are described in the appendix.

Accuracy of data. - The data presented herein show combustion efficiencies as high as 108 percent; obviously, considerable error is present. The errors are attributable to three factors: (1) errors in measurement of fuel temperature (see appendix), which affects fuel density and, hence, fuel-flow rate, (2) oscillating flows and temperatures that existed during

DECLASSIFIED

some of the runs, and (3) large exhaust-gas temperature corrections that were subject to error (see appendix). The measured variables oscillated at 1 to 2 cycles per minute at a relatively high amplitude. The data were recorded at both the maximum and minimum values of the cycle. Since all the variables appeared to reach the maximum and minimum values at the same time, each extreme of the cycling was considered to be a separate point in the calculations.

RESULTS AND DISCUSSION

The performance data obtained with the J33 and the vaporizer-tube combustors are presented in tables I and II, respectively. Data relating to the operation of the fuel system are also included in the tables.

Combustor Performance

Combustion efficiency. - The combustion efficiencies of the J33 combustor with gaseous hydrogen fuel at ambient temperatures are shown in figure 10. In general, efficiencies from approximately 95 to 100 percent were obtained at all operating conditions investigated. The few data points that fall above 100 percent indicate the probability that the radiation corrections applied to the outlet thermocouples were in error. The combustion efficiencies of the J33 combustor with cold fuel are presented in figure 11. The greater scatter of the data is due to inaccuracies in the flow and temperature measurements with the cold fuel, as previously discussed. There appears to be no relation between the combustion-efficiency level and the fuel temperature (indicated at each data point). The fuel temperatures shown in figure 11 were measured at the outlet of the orifice run with a bare-wire thermocouple.

Comparison of figure 11 with figure 10 indicates that the large change in fuel temperature apparently had no effect on combustion efficiency. The efficiency level is near 100 percent even at the lowest pressure condition of 4 inches of mercury absolute.

The combustion efficiencies obtained with the vaporizer-tube combustor are presented in figure 12. The performance is similar to that obtained with the J33 combustor; efficiencies were near 100 percent and there was no apparent relation between efficiency and fuel temperature. The data of figure 12(a) were obtained at a reference velocity of 191 feet per second as compared with 68 and 60 for figures 12(b) and (c), respectively.

Vaporizer-tube temperatures. - Temperatures of the mixture of air and cold hydrogen fuel flowing through the vaporizer tube, as well as the vaporizer-tube wall temperatures, are presented in figure 13. The gas

temperature was measured at three stations (1, 2, and 3), as shown in the sketch in figure 13. Most of the data were beyond the range (-100° to 700° F) of the instrument used to indicate the temperature. Station 1 temperatures are plotted in figure 13(a). Three data points at -100° F indicate that the temperature was -100° F or lower. The other two data points show the increase in gas temperature with an increase in fuel temperature. Temperatures measured at stations 2 and 3 were always above 700° F, the maximum reading of the instrument. These data indicate two possible occurrences: (1) a small flame may have existed in the tube between stations 1 and 2, causing the large temperature rise, or (2) the thermocouples at stations 2 and 3 may have been influenced by conduction and radiation from the tube walls.

Attempts were made to correlate vaporizer-tube wall temperatures with combustor outlet temperature, fuel flow, and fuel temperature entering the tube. The data indicated a much better correlation with fuel temperatures than with either of the other two variables. The data are shown in figure 13(b). These data (fig. 13) indicate that, if a hydrocarbon fuel and cold hydrogen are injected simultaneously into the vaporizer tube, the hydrocarbon could possibly freeze; but it is unlikely that any build-up of solid fuel would occur, since the tube wall temperatures are high.

Temperature profile. - The temperature patterns at the outlet of the J33 combustor for both warm- and cold-fuel operation are presented in figure 14. The data used for developing the isotherms in the figure are not included in the data table. Fuel temperature had no apparent effect on outlet temperature profiles; the differences that do exist are probably due to the difference (146° F) in the average exhaust-gas temperature. The profiles were similar to those obtained with hydrocarbon fuels in this combustor. The temperature patterns at other test conditions were similar to those presented in figure 14.

A typical temperature pattern measured at the outlet of the vaporizing-tube combustor is presented in figure 15. This combustor produced a hot region in the center of the duct. The difference between the maximum and the minimum temperatures is about 800° F as compared with about 400° F for the J33 combustor (fig. 14(a)). No design changes were made to reduce the temperature gradient.

Fuel System

Qualitative observations, together with limited quantitative data relating to the design and operation of the liquid-hydrogen fuel system, are described in the following paragraphs.

Fuel-system temperature. - The temperature of the hydrogen fuel at various stations in the fuel system from the outlet of the concentric-tube heat exchanger to the fuel feed tubes in the vaporizer-tube combustor

is shown in figure 16 as a function of fuel-flow rate. These data were obtained with the fuel system arranged as shown in figure 8(a). The data of figure 16(a) were obtained with the fuel flowing through the bypass, around the tailpipe heat exchanger, directly into the combustor. The lowest curve (A) represents the fuel temperature at the outlet of the concentric-tube heat exchanger, where the fuel temperature is slightly above its boiling temperature. The temperature difference between curve A and curve B represents the heat leak into approximately 16 feet of vacuum-insulated transfer pipe plus the heat leak into the orifice run. The temperature difference between curves B and C represents the heat leak into the fuel line between the orifice-run outlet and the inlet of the fuel feed tube in the combustor (30 in.). Since the length of the line from the orifice to the fuel feed tube is about the same as the length of the orifice run, and since the temperature difference between A and B is about the same as between B and C, the heat leak into the vacuum-insulated pipe was very small. A substantial temperature rise (C to D) occurred in the 3.5-inch-long fuel feed tubes; these tubes were immersed in the 300° F combustor inlet air.

Fuel temperatures obtained with the fuel flowing through the tailpipe heat exchanger (fig. 8) are shown in figure 16(b). As would be expected, the largest temperature increase is in the tailpipe heat exchanger.

The effectiveness of the vacuum-insulated transfer pipe in preventing heat leak into the liquid hydrogen could be calculated from the fuel-system data obtained. The fuel temperature at the inlet to the concentric-tube heat exchanger is plotted against fuel flow in figure 17. The fuel temperature remains constant to a minimum flow of 5 pounds per hour. At this point, the heat-leak rate into the pipe is sufficient to vaporize all of the flowing fuel. This accounts for the increase in fuel temperature at fuel flows below 5 pounds per hour. The scatter in the data is due primarily to the variable pressure in the fuel line and to possible errors in the temperature measurement. From the data obtained at minimum fuel-flow rates, the heat-leak rate was calculated to be approximately 38 Btu per hour per foot of length.

Fuel-system oscillations. - The hydrogen fuel, supplied as a liquid, boiled or flashed into a vapor either in the heat exchanger or in the transfer piping. Oscillations occurred in the fuel system downstream of the station where boiling occurred. These oscillations affected the fuel pressure, temperature, and flow rate, and combustor outlet temperatures. A recording made of the fuel temperature at three different stations in the fuel system is presented in figure 18. The temperature of the liquid hydrogen entering the concentric-tube heat exchanger was constant at its equilibrium temperature; whereas, the temperature at the outlet of the heat exchanger oscillated between the liquid temperature (-416° F) and -400° F. The temperature variations at the fuel-orifice

run are shown in figure 18 for a high and a low fuel-flow rate. The amplitude of the oscillations at the high flow rate was about three times that at the lower flow rate. The frequency of the oscillations shown in figure 18 is approximately 1 cycle per minute. Other data showed slightly higher frequencies; the frequency is probably a function of the dynamics of the fuel system, which would vary with design.

During operation, it was noted that fuel pressure, temperature, and orifice pressure drop varied in unison; that is, when the pressure was at a maximum, the temperature would be at a low value and the pressure drop across the orifice would be at a high value. Thus, the fuel density varied over a large range, causing large variations in fuel flow during the oscillation. Several attempts were made to control the oscillation by making design changes in the fuel system. The original fuel system had a length of pipe of negative slope following the heat exchanger. If the liquid fuel periodically spilled over into the lower section of the system and vaporized at the bottom, oscillations could occur. The transfer pipe was relocated so that the fuel flowed uphill over most of the distance to the combustor. This change did not eliminate the oscillation; however, the combustor temperature variations were less erratic.

Liquid hydrogen has a very low density and low viscosity, and thus low inherent damping characteristics. For this reason, additional restrictions to fluid flow were installed at several points in the fuel system in an attempt to eliminate the oscillation. Seven 8-foot lengths of 3/16-inch copper tubes with the ends sealed off were installed inside the concentric-tube heat exchanger. The amplitude of the oscillations at the highest flow rates was reduced; however, oscillations still existed in the middle flow range. Next, fuel velocity in the system was increased by operating at a lower pressure level. A check valve designed to maintain a line pressure 20 pounds per square inch lower than the Dewar pressure was installed in the liquid-hydrogen fuel line near the Dewar tank. Approximately half the data reported herein were obtained with this valve installed. The fuel flows were relatively stable in the lowest and the highest 25 percent of the over-all fuel-flow range. Oscillations were still encountered in the middle 50 percent of the range. In the high flow range, a change in fuel-flow setting would cause the oscillations to reoccur; they would, however, slowly diminish with time.

A brief study was made with an automatic, piston-operated valve installed in the fuel line close to the orifice run. The pressure downstream of the valve was regulated equal to a control pressure signal supplied to the piston independent of the variable upstream pressure. This control method worked well, but difficulty was encountered in preventing leaks through the shaft seals of the valve.

Finned-tube heat exchanger. - The finned-tube heat exchanger was a compact design for adding heat to vaporize liquid hydrogen. Tests were

conducted to determine the effect of rapid temperature changes on the unit. The unit, which was immersed in a 1500° F gas stream, was subjected to rapid cooling by introducing into it hydrogen gas at -400° F. Examination of the tube after several trials showed no damage that could be attributed to the thermal shock.

SUMMARY OF RESULTS

The results of a brief study of turbojet combustor performance and of fuel-system variables with hydrogen at a temperature near its boiling point are summarized as follows:

1. Combustion efficiencies near 100 percent were obtained for two different combustor designs over a range of combustor inlet pressures from 4 to 40 inches of mercury absolute. Similar results were obtained with fuel at ambient temperatures, indicating no significant effects of fuel temperature on combustion efficiency.
2. Combustor outlet temperature profiles were not adversely affected by the low fuel temperature.
3. Control and measurement of fuel-flow variables showed that pressure and temperature oscillations occurred in the two-phase portion of the cold-hydrogen-fuel system.
4. The rate of heat leak into a vacuum-insulated transfer pipe was calculated to be approximately 38 Btu per hour per foot of length.
5. No noticeable damage occurred in a finned-tube heat exchanger that was subjected to cold-fuel introduction at fuel temperatures near -400° F while immersed in a 1500° F gas stream.

Lewis Flight Propulsion Laboratory
National Advisory Committee for Aeronautics
Cleveland, Ohio, November 26, 1956

APPENDIX - CALIBRATION

The copper-constantan thermocouple wire used for fuel temperature measurement was calibrated at three temperature reference points: liquid hydrogen, liquid nitrogen, and ice water. The method used to obtain a complete calibration curve is illustrated in figure 19. Data for copper-constantan thermocouples reported in reference 6 were used as a basis. The data were plotted on semilogarithmic paper and adjusted empirically until a straight-line calibration was obtained. Two different scale factors had to be used to linearize the data, as shown in figure 19. The data obtained with two different thermocouples reported in reference 6 were linearized by the same scale factor at temperatures below 130° R.

The low temperatures measured in this investigation were indicated by millivolt readings obtained on a slide-wire potentiometer with a reference bath of liquid nitrogen. For liquid hydrogen and with the liquid-nitrogen bath, the millivolt variation per degree change in temperature was small, approximately -0.006 millivolt per °R. Millivolt readings were obtained with the thermocouple immersed in the liquid hydrogen at the inlet side of the concentric-tube heat exchanger. The temperature of the hydrogen was assumed to be the equilibrium temperature at the pressure existing in the flow system. Twelve of these data points are shown in figure 19. Since the other two curves were linear between 40° and 140° R, it was assumed that the thermocouples being calibrated were also linear in this range with the scale factor chosen. At temperatures above 130° R, the calibration differences were negligible. The scatter of the data points indicates an error of approximately $\pm 2^\circ$ R due to drift in the potentiometer. When the calibration was completed, the data were replotted on rectilinear coordinates similar to those shown in figure 20. In the example shown, the millivolt readings were corrected to a reference temperature of ice water.

The possible error due to thermocouple calibration is illustrated in figure 20. A difference of approximately 10° R may be obtained at the same millivolt reading of -6.15 millivolts. In this temperature range (40° R), this represents a 25-percent difference in absolute temperature due to thermocouple calibration alone.

The effect of shielding the thermocouple used in the orifice run is illustrated in figure 21. Original calculations showed that indications from bare-wire thermocouples in the cold stream may be erroneously high by approximately 5° R owing to radiation from the surrounding tube. The data presented in figure 21, however, show that the bare-wire thermocouple in most cases indicated lower temperatures than the shielded thermocouple, particularly at lower temperatures approaching liquid-hydrogen temperature. The indicated temperature differences were, in most cases, no greater than $\pm 4^\circ$ R, representing about ± 8 percent at the lowest temperature of 50° R and about ± 2 percent at 230° R. These differences may be attributed

to the drift in the potentiometer and to the reading error. They cannot be attributed to heat added to the system between the two thermocouples, because the bare-wire thermocouple was installed about 1 inch downstream of the shielded thermocouple.

Fuel-Flow Measurement

The following equation was used for calculating fuel flows:

$$w_f = 358.9 d_2^2 C_{f1} Y E \sqrt{\rho \Delta P}$$

where

w_f fuel-flow rate, lb/hr

d_2 orifice diameter, in.

C_{f1} over-all flow coefficient, dimensionless

Y expansion factor, dimensionless

E area multiplier for thermal expansion, dimensionless

ρ fluid density, lb/cu ft

ΔP differential pressure drop (in water)

Most of the terms in the equation are affected by variations in properties of the hydrogen fuel at the low temperatures. The flow coefficient C_{f1} is constant over most of the range of fuel flows but increases quite rapidly at low Reynolds numbers. Some of the data obtained were in this low Reynolds number region. The viscosity of cold hydrogen varies markedly with temperature and had to be accounted for in the calculation of Reynolds number. Since the incompressible-flow equation was used, the factor Y was introduced to account for the expansion of the gases following the orifice. The term Y is affected by the ratio of specific heats of the fluid as well as the pressure ratio across the orifice. The ratio of specific heats of hydrogen varies considerably at temperatures below ambient, as shown in figure 22 (ref. 7). Most of the data reported were at fuel temperatures in the region where the ratio of specific heats was constant at 1.67. Some of the data, however, were in the temperature range above 100° R, where the ratio varies with temperature and also depends on the form (ortho or para) of hydrogen. Under standard temperature and pressure conditions, hydrogen exists in the ratio of three parts ortho to one part para; however, at very low temperatures all hydrogen

molecules tend to convert to the para form. Since the proportion of ortho- and para-hydrogen supplied to the fuel system was not known, the intermediate, "normal" curve shown in figure 22 was used in the calculations.

The area correction factor E in the flow equation affected flow rate by only about 0.5 percent, which was negligible compared with the effects of the other variables. The density of the hydrogen ρ at temperatures near the boiling point deviates somewhat from the perfect gas laws. The densities, therefore, were read from a chart (ref. 7).

Combustor Outlet Temperature

The 25 thermocouples used to measure combustor outlet temperatures were arranged in three rings, each containing eight thermocouples and one located in the center of the duct. The thermocouples were designed with a long length-to-diameter ratio to minimize conduction error (ref. 5). Radiation corrections were applied to the average thermocouple readings by the method of reference 5. Unpublished data obtained in combustion tests with hydrogen indicated that the radiation correction could be applied to the average of the individual readings rather than to each thermocouple reading individually. Values of radiation correction in tables I and II were as high as 405° F at the highest temperature level. These large corrections are themselves subject to appreciable error because of limited wall temperature data used to calculate this correction.

REFERENCES

1. Silverstein, Abe, and Hall, Eldon W.: Liquid Hydrogen as a Jet Fuel for High-Altitude Aircraft. NACA RM E55C28a, 1955.
2. Jonash, Edmund R., Smith, Arthur L., and Hlavin, Vincent F.: Low-Pressure Performance of a Tubular Combustor with Gaseous Hydrogen. NACA RM E54L30a, 1955.
3. Wear, Jerrold D., and Smith, Arthur L.: Performance of a Single Fuel-Vaporizing Combustor with Six Injectors Adapted for Gaseous Hydrogen. NACA RM E55I14, 1956.
4. Sivo, Joseph N., and Fenn, David B.: Performance of a Short Combustor at High Altitude Using Hydrogen Fuel. NACA RM E56D24, 1956.
5. Scadron, Marvin D., and Warshawsky, Isidore: Experimental Determination of Time Constants and Nusselt Numbers for Bare-Wire Thermocouples in High-Velocity Air Streams and Analytic Approximation of Conduction and Radiation Errors. NACA TN 2599, 1952.

REF ID: A57150

6. Swenson, C. A., and Basinski, Z. S.: Thermocouple Calibrations, 4.2° to 273.2° K. Tech. Rep. No. 2, Paper No. 3, Dept. Mech. Eng., Cryogenic Lab., M.I.T., May 23, 1952 to July 31, 1955. (Office Ord. Res., Contract No. DA-19-020-ORD-1891, Ord. Proj. No. TB 2-0001 (539).)
7. Woolley, Harold W., Scott, Russell B., and Brickwedde, F. G.: Compilation of Thermal Properties of Hydrogen in Its Various Isotropic and Ortho-Para Modifications. Jour. Res. Nat. Bur. Standards, vol. 41, no. 5, Nov. 1948, pp. 379-455.

TABLE I. - EXPERIMENTAL DATA FOR J33 COMBUSTOR

Run	Combustor inlet total pressure, in. Hg abs	Combustor inlet total temperature, °F	Air flow rate, lb/sec	Combustor reference velocity, ft/sec	Fuel flow, lb/hr	Fuel/air ratio	Average combustor outlet temperature uncorrected for radiation, °F	Average combustor outlet temperature corrected for radiation, °F	Combustion efficiency, percent	Combustor outlet pressure, in. Hg abs	Fuel pressure in heat exchanger, in. abs	Fuel temperature in heat exchanger inlet, °F	Fuel temperature in heat exchanger outlet, °F	Helium flow rate in heat exchanger, lb/hr	Helium inlet temperature, °F	Helium outlet temperature, °F	Outdoor ambient temperature, °F
1	15.0	504	0.678	98	9.01	0.0037	985	1019	100.8	14.1	61.42	-414	-338	-266	52	---	34
2	15.0	508	.678	96	9.47	.0039	1015	1051	99.8	14.1	61.42	-414	-350	-284	52	---	34
3	15.0	500	.678	97	15.28	.0065	1550	1452	98.8	14.0	59.42	-414	-408	-345	52	---	34
4	15.0	296	.680	97	14.92	.0061	1545	1425	100.5	14.0	58.42	-415	-393	-346	52	---	34
5	15.2	295	.679	95	15.85	.0061	1560	1680	98.5	14.1	53.42	-414	-383	-345	52	---	34
6	50.0	292	1.534	98	15.00	.0030	900	916	106.5	28.2	61.42	-414	-414	-374	52	---	34
7	15.1	295	---	---	---	---	---	---	---	---	---	-416	---	-347	52	---	34
8	50.0	296	1.390	99	18.06	.0042	920	950	101.6	28.1	55.26	-419	-404	-396	9.36	48	46
9	50.0	296	1.390	---	19.25	.0059	1055	1058	103.5	28.1	55.26	-420	-419	-396	9.36	48	46
10	50.1	297	1.370	97	21.85	.0044	1100	1115	97.9	28.6	58.26	-419	-418	-396	10.31	49	46
11	50.7	297	1.370	---	29.16	.0059	1270	1509	93.2	28.9	58.26	-419	-395	-411	10.31	49	46
12	29.2	293	1.385	101	32.17	.0064	1355	1359	90.7	27.3	60.26	-415	-402	-398	16.69	51	46
13	50.1	297	1.385	---	34.37	.0069	1550	1615	98.2	28.2	62.26	-415	-415	-397	17.40	52	46
14	29.9	297	1.400	100	31.65	.0065	1455	1478	103.1	27.8	60.4	-422	-422	-383	10.29	41	-256
15	50.1	296	1.410	100	45.25	.0065	1750	1656	103.5	28.0	69.4	-422	-422	-394	14.34	45	-245
16	50.0	297	1.412	101	---	.0026	820	827	102.4	28.3	66.7	-420	-420	-380	4.56	---	28
17	15.0	294	.640	91	13.45	.0059	1300	1385	100.6	14.1	66.4	-420	-418	-380	4.56	---	28
18	15.1	296	.686	97	120.95	.0065	1655	1771	99.0	14.0	26.45	---	---	-382	---	55	28
19	50.0	297	1.425	102	30.19	.0059	1355	1375	99.6	28.0	30.95	-417	-417	-368	6.16	49	-99
20	50.2	280	1.402	97	30.99	.0061	1375	1426	101.7	28.3	50.4	-420	-394	-361	---	---	28
21	50.1	277	1.405	98	30.13	.0059	1350	1372	100.0	28.1	---	-422	-370	-344	17.80	46	-196
22	50.1	303	1.414	101	30.22	.0060	1355	1378	97.9	28.1	51.12	-416	-371	-397	16.25	46	-196
23	50.1	298	1.414	101	30.15	.0059	1355	1376	98.7	28.3	45.12	-420	-405	-380	8.26	44	-202
24	8.0	506	.569	100	5.71	.0043	1055	1116	99.0	7.5	69.1	---	---	-296	---	---	---
25	7.8	297	.370	102	15.85	.0115	1912	2296	104.2	7.1	26.45	-419	-419	-370	---	---	60
26	8.1	292	.357	94	8.50	.0066	1350	1486	98.6	7.1	62.1	-410	-318	-276	---	---	42
27	8.1	293	.362	95	12.76	.0098	1650	1862	98.4	7.0	58.1	-412	-378	-332	---	---	42
28	7.8	305	.361	100	7.81	.0060	1280	1354	95.3	7.2	45.6	-417	-351	-294	---	---	42
29	8.1	295	.360	95	13.70	.0106	1750	1914	90.1	7.0	41.1	-416	-376	-354	---	---	36
30	3.8	309	.214	122	3.40	.0044	1030	1084	92.6	3.4	44.1	-379	-264	-242	---	---	36
31	8.1	310	.362	97	3.52	.0027	905	828	97.1	7.6	72.9	-382	-344	-291	---	---	36
32	8.1	300	.355	94	7.03	.0055	1205	1286	96.5	7.7	59.4	---	---	-344	---	---	36
33	4.0	295	.255	125	2.49	.0029	835	874	100.1	3.6	62.4	-362	-316	-249	---	---	36
34	4.1	296	.232	121	2.51	.0052	1155	1287	101.9	3.7	55.4	-403	-377	-296	---	---	36
35	4.0	295	.250	123	6.53	.0078	1470	1694	100.9	3.6	58.9	---	-414	-337	---	---	36
36	4.0	295	.253	124	4.10	.0049	1140	1229	101.9	3.5	64.4	-396	-374	-312	---	---	36
37	3.9	297	.233	125	3.12	.0037	965	1016	100.5	3.5	64.4	-378	-351	-304	---	---	36
38	4.0	301	.253	126	1.68	.0020	705	715	104.0	3.6	65.4	-360	-322	-273	---	---	36
39	4.1	297	.236	123	7.94	.0093	1655	1933	101.6	3.6	47.4	-420	-378	-336	---	---	36
40	14.9	290	.668	95	4.98	.0021	670	683	96.6	14.2	---	---	---	65.5	---	---	36
41	15.1	290	.668	94	8.29	.0034	912	942	97.1	14.3	---	---	---	65.5	---	---	---
42	15.1	500	.668	95	11.32	.0047	1115	1170	97.6	14.2	---	---	---	69.0	---	---	---
43	15.1	292	.668	94	14.19	.0059	1295	1378	99.3	14.2	---	---	---	73	---	---	---
44	15.1	294	.668	94	16.26	.0068	1420	1522	99.7	14.1	---	---	---	77	---	---	---
45	7.8	291	.352	96	2.63	.0021	685	707	97.9	7.4	---	---	---	79	---	---	---
46	8.0	288	.351	93	4.34	.0034	910	962	100.6	7.5	---	---	---	84	---	---	---
47	7.8	306	.347	96	5.84	.0047	1095	1174	97.2	7.3	---	---	---	84	---	---	---
48	8.1	307	.351	94	8.42	.0067	1340	1484	96.4	7.6	---	---	---	87	---	---	---
49	7.8	307	.345	96	10.55	.0085	1550	1765	97.0	7.2	---	---	---	90	---	---	---
50	7.9	305	.338	93	12.93	.0106	1770	2011	93.3	7.3	---	---	---	91	---	---	---
51	8.0	307	.350	95	6.58	.0052	1195	1274	98.2	7.6	---	---	---	93	---	---	---
52	4.0	289	.234	124	1.50	.0018	645	655	101.3	3.5	---	---	---	93	---	---	---
53	4.0	292	.234	124	2.55	.0030	820	868	102.3	3.5	---	---	---	91	---	---	---
54	4.0	293	.234	125	2.87	.0034	880	935	92.5	3.6	---	---	---	85	---	---	---
55	4.0	295	.234	125	4.07	.0048	1070	1169	95.4	3.6	---	---	---	84	---	---	---
56	4.0	299	.234	126	5.88	.0070	1335	1522	96.3	3.5	---	---	---	80	---	---	---
57	4.1	293	.234	121	7.09	.0084	1505	1760	98.5	3.6	---	---	---	82	---	---	---
58	4.0	295	.234	125	8.82	.0105	1725	2095	100.0	3.5	---	---	---	86	---	---	---
59	3.9	293	.234	128	4.82	.0057	1215	1332	97.0	3.4	---	---	---	91	---	---	---
60	15.1	293	.680	96	4.97	.0020	685	695	99.2	14.5	---	---	---	54	---	---	---
61	14.9	294	.680	97	10.06	.0041	1050	1088	101.3	14.1	---	---	---	47	---	---	---
62	15.0	296	.680	97	16.38	.0067	1420	1516	100.9	14.0	---	---	---	46	---	---	---
63	15.0	296	.680	97	21.51	.0088	1670	1819	99.1	14.0	---	---	---	45	---	---	---
64	4.0	176	.245	110	5.74	.0055	1175	1301	95.2	3.4	---	---	---	37	---	---	---
65	4.0	176	.245	110	2.09	.0024	615	631	97.3	3.6	---	---	---	42	---	---	---
66	4.0	177	.245	110	8.24	.0105	1650	1989	100.1	3.5	---	---	---	40	---	---	---
67	4.0	176	.245	110	10.04	.0118	1800	2205	101.7	3.5	---	---	---	40	---	---	---

TABLE II. - EXPERIMENTAL DATA FOR VAPORIZER-TUBE COMBUSTOR

Run	Combustor inlet total pressure, in. Hg abs	Combustor inlet total temperature, °F	Air flow rate, lb/sec	Combustor reference velocity, ft/sec	Fuel flow, lb/hr	Fuel-air ratio	Average combustor outlet temperature uncorrected for radiation, °F	Average combustor outlet total temperature corrected for radiation, °F	Combustion efficiency, percent	Combustor outlet total pressure, in. Hg abs
1	15.1	296	0.675	95	21.18	0.0087	1710	1934	107.6	14.2
2	15.2	300	.685	97	16.34	.0049	1145	1211	98.6	14.2
3	40.6	299	1.110	60	26.3	.0080	1490	1595	91.0	39.3
4	39.6	298	1.134	61	14.96	.0037	975	1003	100	38.7
5	36.4	298	1.324	78	20.11	.0042	1110	1156	106.2	35.1
6	36.4	298	1.127	66	9.01	.0022	720	730	98.0	35.5
7	36.9	296	1.165	67	9.64	.0023	710	720	93.3	36.0
8	37.0	296	1.139	66	17.68	.0043	1020	1044	90.2	36.1
9	37.0	296	1.139	66	15.92	.0039	1020	1075	104.6	36.1
10	36.8	298	1.175	69	20.22	.0048	1150	1174	96.3	35.7
11	36.9	298	1.246	72	12.39	.0028	830	800	89.9	35.9
12	36.2	294	1.100	65	20.98	.0053	1230	1267	97.6	35.2
13	14.3	295	1.296	193	24.87	.0053	1225	1272	98.0	9.5
14	14.2	298	1.264	192	31.00	.0068	1425	1513	97.9	9.5
15	13.0	296	1.175	193	23.08	.0055	1200	1246	92.4	8.7

Run	Fuel pressure in fuel supply line, lb/sq in. abs	Fuel temperature orifice run, °F	Tailpipe heat-exchanger inlet fuel temperature, °F	Tailpipe heat-exchanger outlet fuel temperature, °F	Fuel injector inlet fuel temperature, °F	Fuel injector outlet fuel temperature, °F	Gas temperature inside of vaporizer tube, station 1, °F	Gas temperature inside of vaporizer tube, station 2, °F	Vaporizer tube wall temperature, °F
1	27.7	-303	----	----	----	----	-----	----	---
2	18.6	-295	----	----	----	----	-----	----	---
3	28.5	-398	----	----	----	----	-----	----	---
4	27.9	-347	----	----	----	----	-----	----	---
5	27.9	-354	----	----	-298	-244	<-100	>700	746
6	21.7	-291	----	----	-221	-149	-----	>700	1085
7	21.8	-298	----	----	-204	-128	-----	>700	1080
8	36.1	-181	-355	-224	-139	-96	-----	Burned out ↓	-----
9	32.7	-181	-355	-224	-139	-96	-----		960
10	40.5	-174	-329	-261	-152	-98	150		1400
11	29.9	-143	-304	-224	-110	-44	390		1960
12	43.2	-185	-346	-252	-144	-89	0		1470
13	43.7	-231	-404	-273	-202	-158	<-100		1020
14	52.6	-240	-416	-300	-201	-166	<-100		860
15	43.3	-187	-357	-271	-165	-117	-----		1065

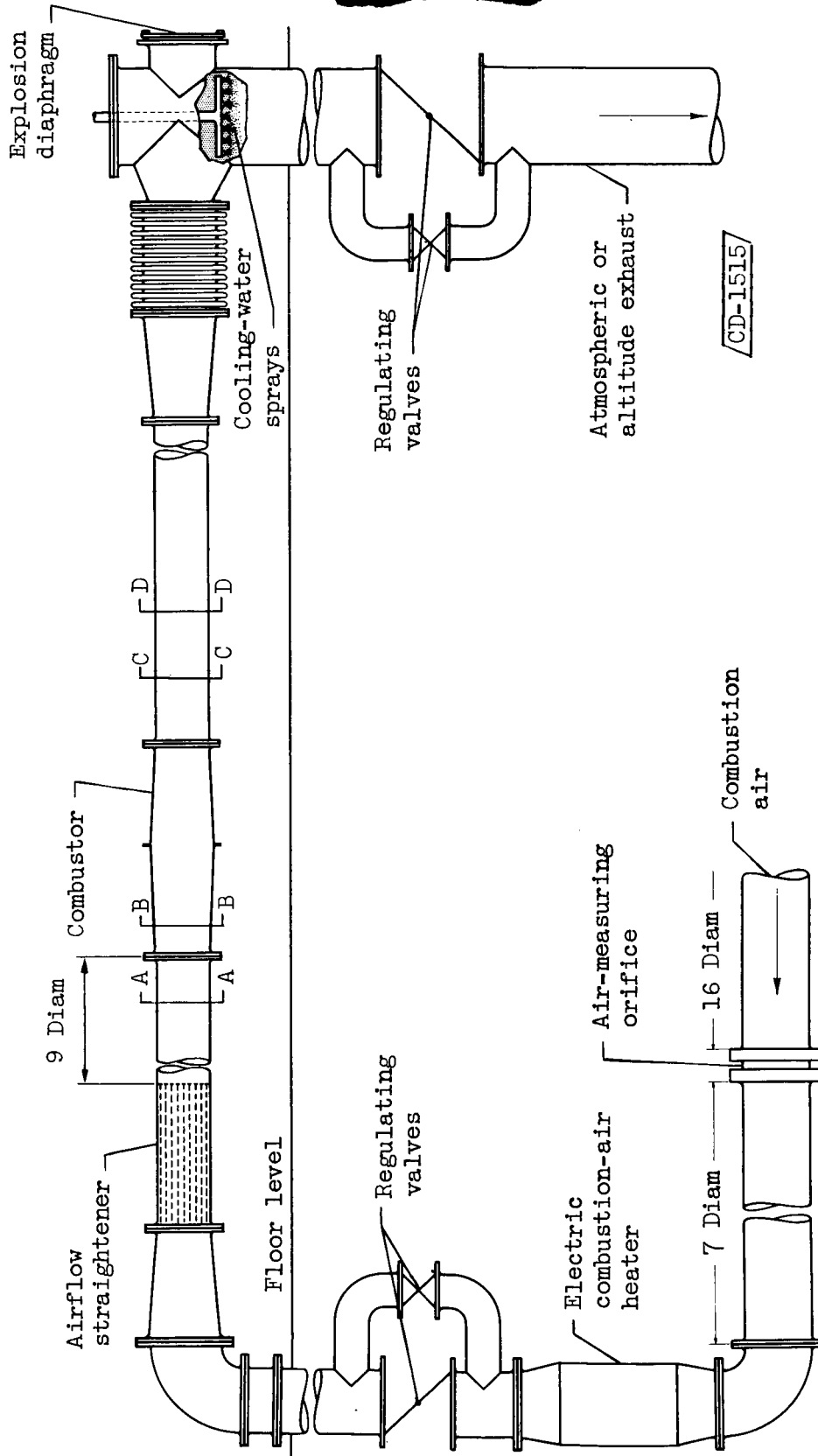


Figure 1. - Single-combustor installation and auxiliary equipment. Instrumentation planes, A-A, B-B, C-C, and D-D.

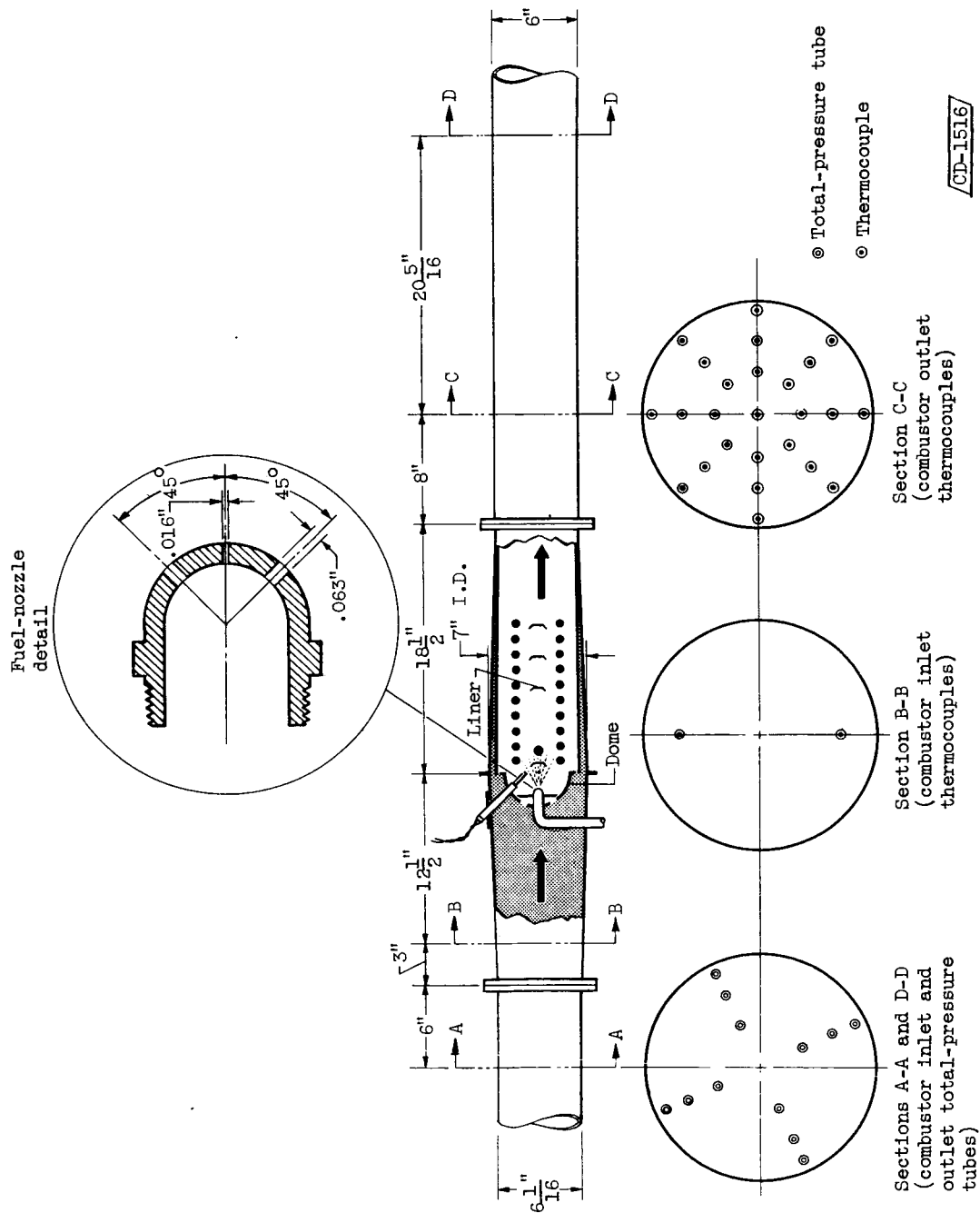


Figure 2. - Cross section of J33 single-combustor installation showing detail of fuel nozzle and location of temperature- and pressure-measuring instruments in instrumentation planes.

037122 133

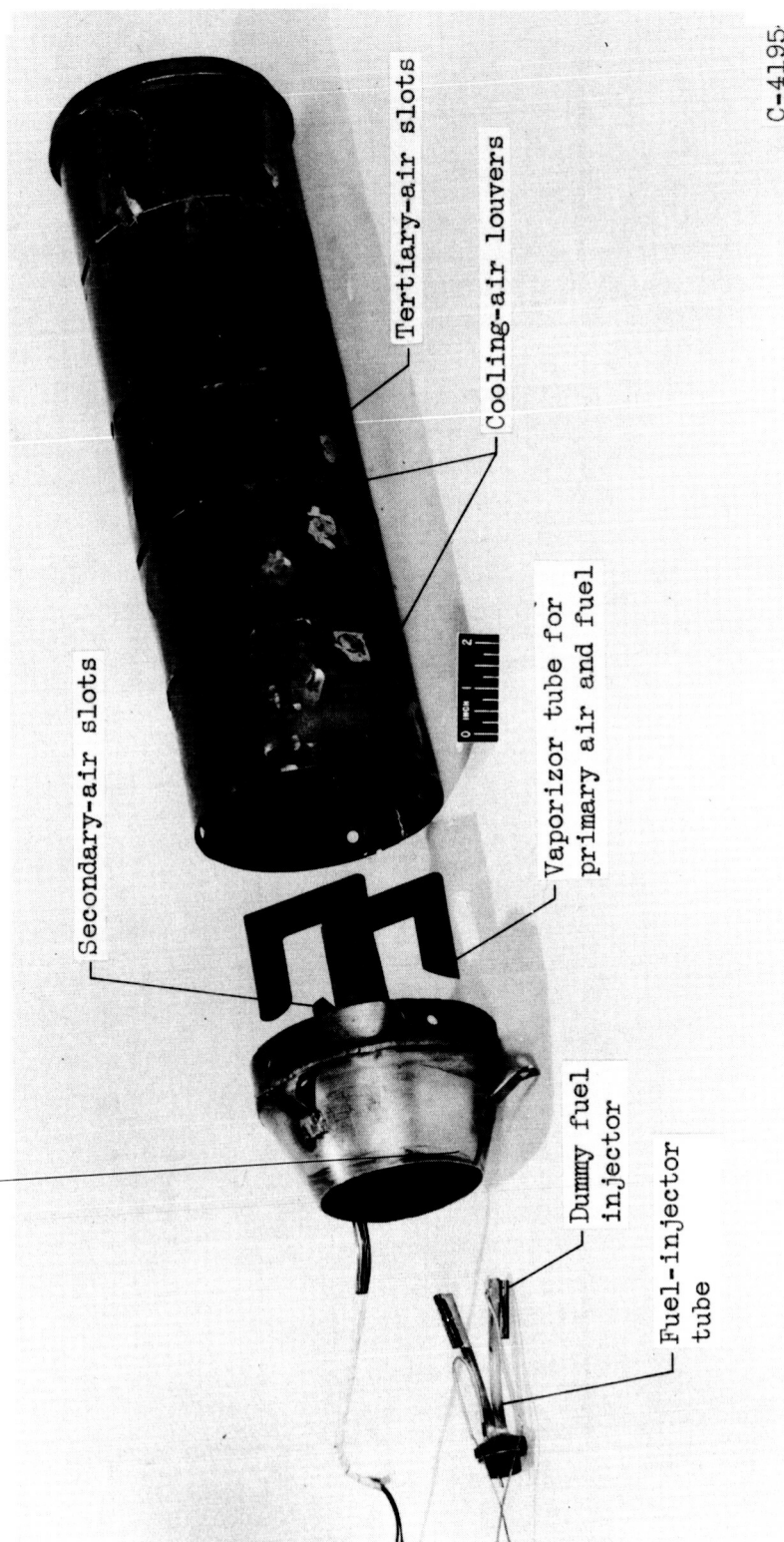


Figure 3. - Vaporizing-tube combustor.

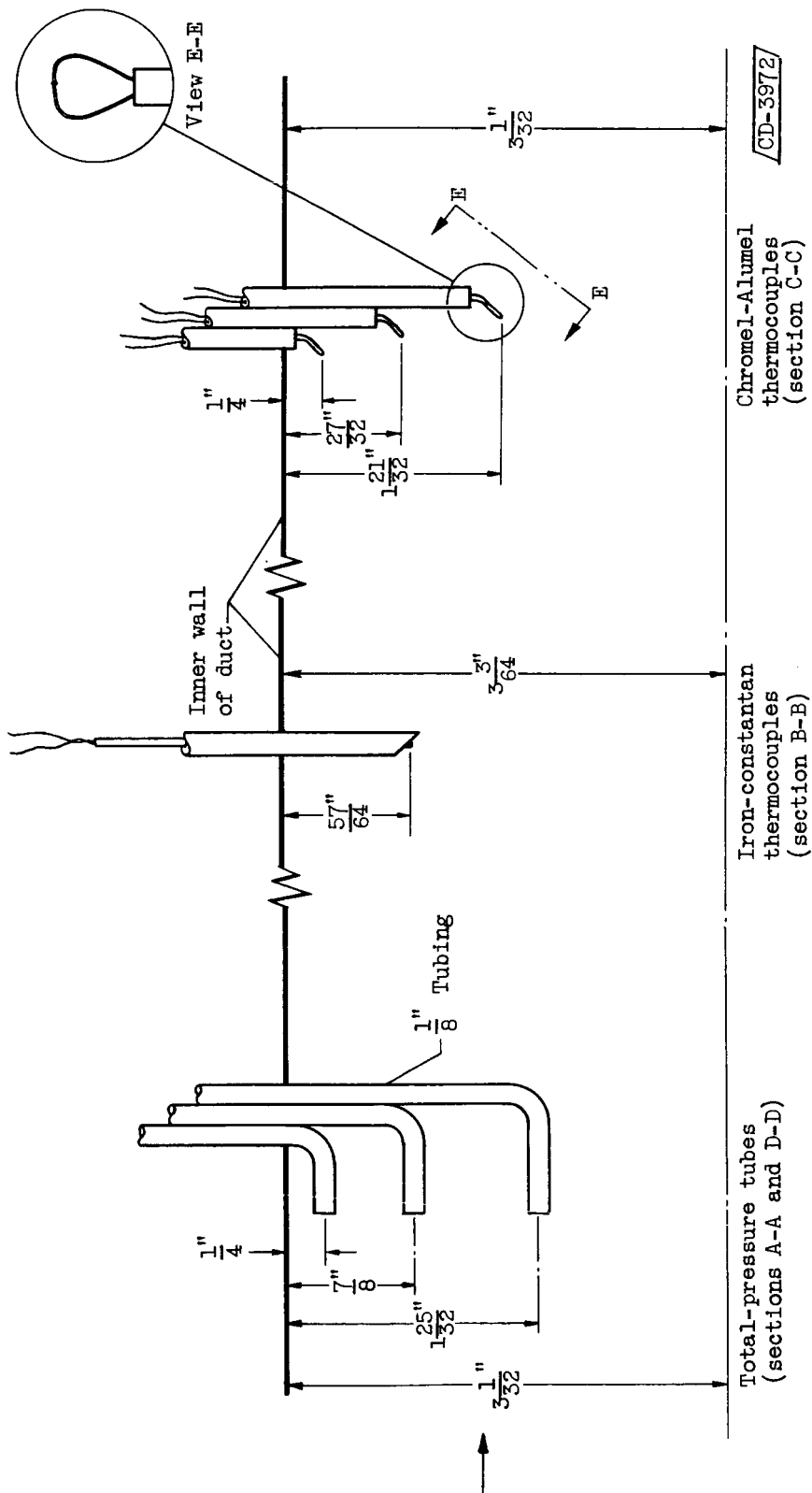


Figure 4. - Construction details of temperature- and pressure-measuring instruments.

4167

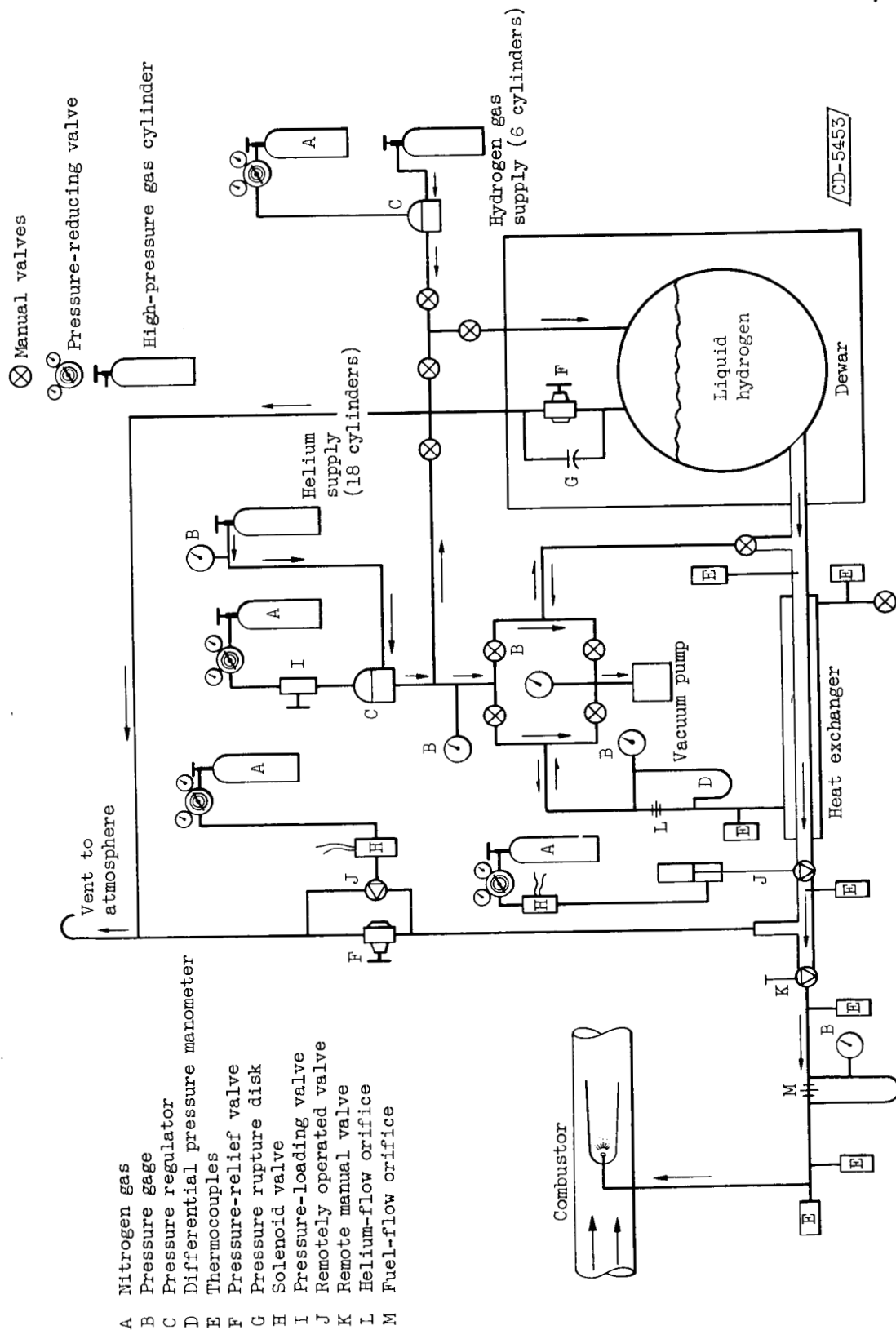


Figure 5. - Schematic diagram of fuel system.

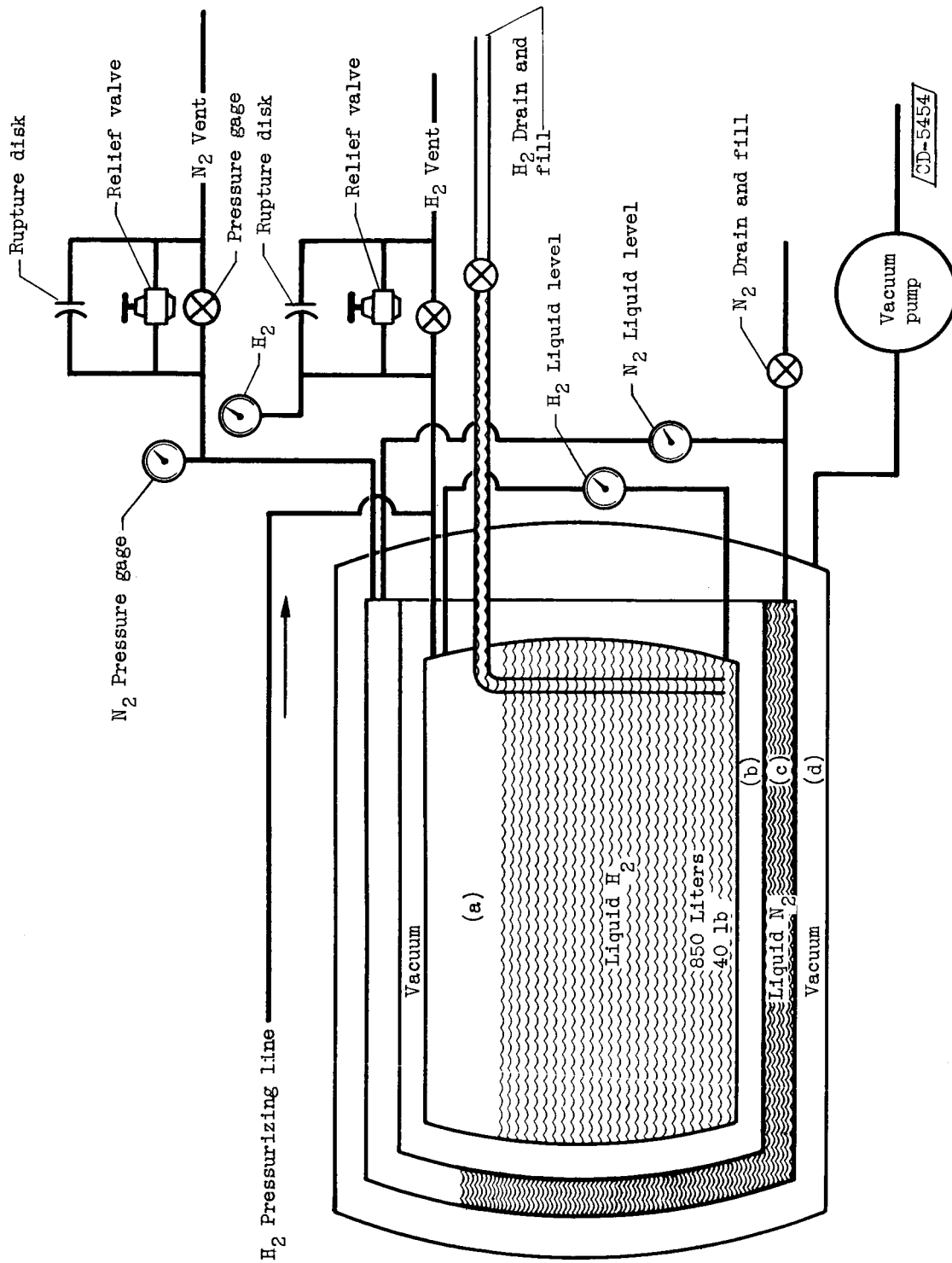


Figure 6. - Schematic diagram of Dewar supply tank for liquid hydrogen, showing some of the associated control equipment.

0371200 1950

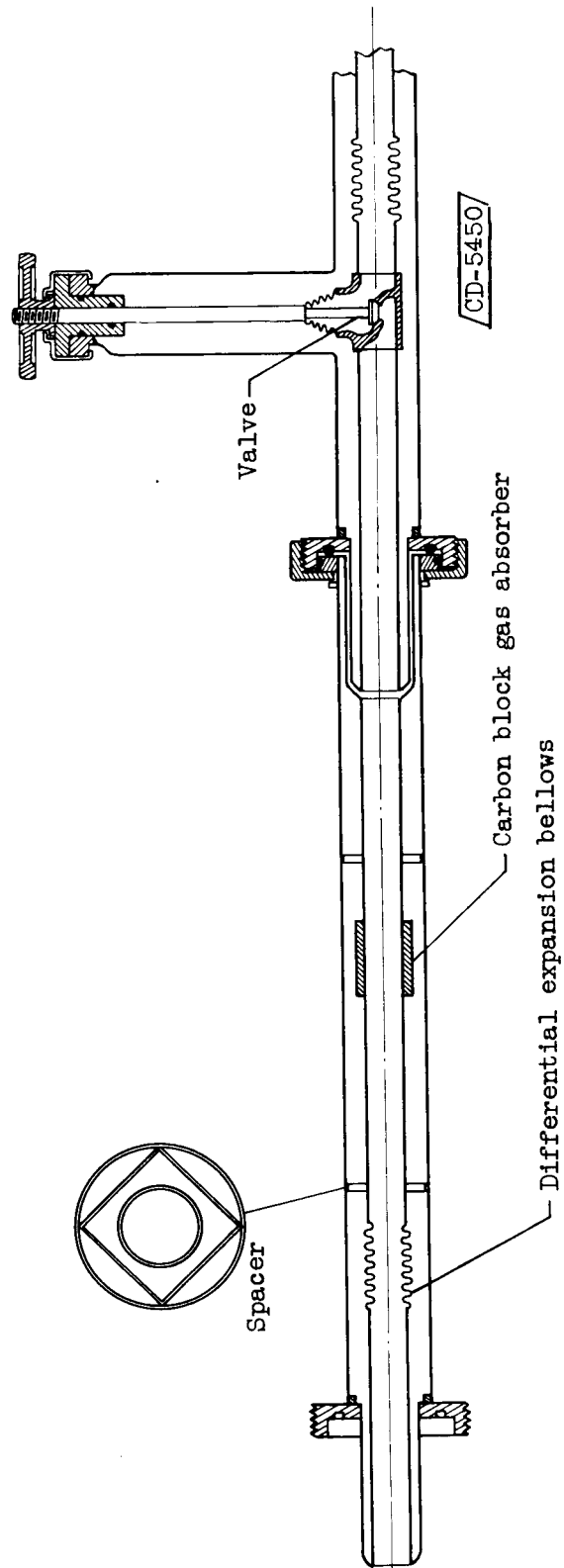
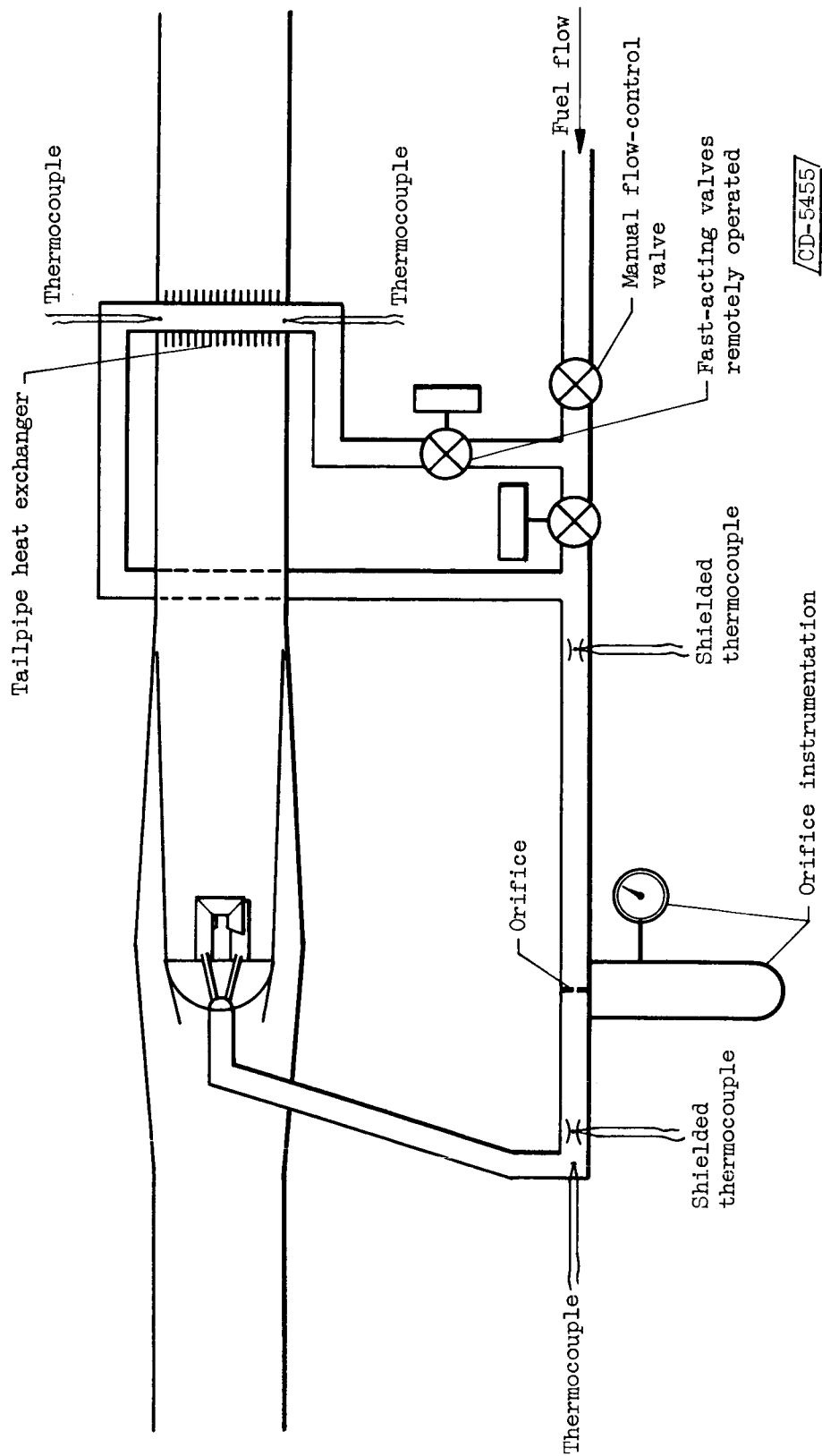


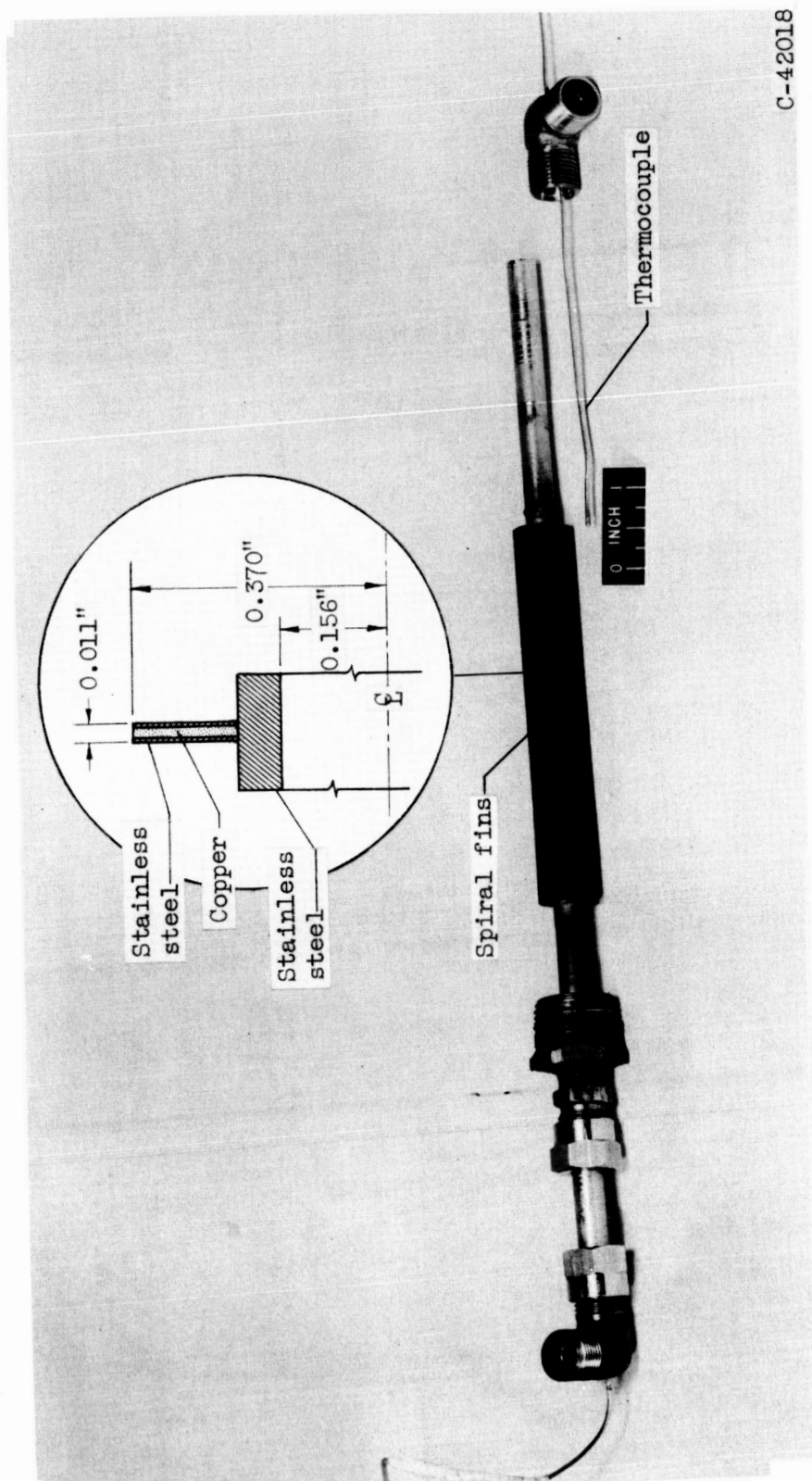
Figure 7. - Schematic drawing of vacuum-insulated fuel line.

CONFIDENTIAL



(a) Schematic diagram of installation.

Figure 8. - Tailpipe heat exchanger and installation in fuel system.



(b) Photograph of finned-tube tailpipe heat exchanger.

Figure 8. - Concluded. Tailpipe heat exchanger and installation in fuel system.

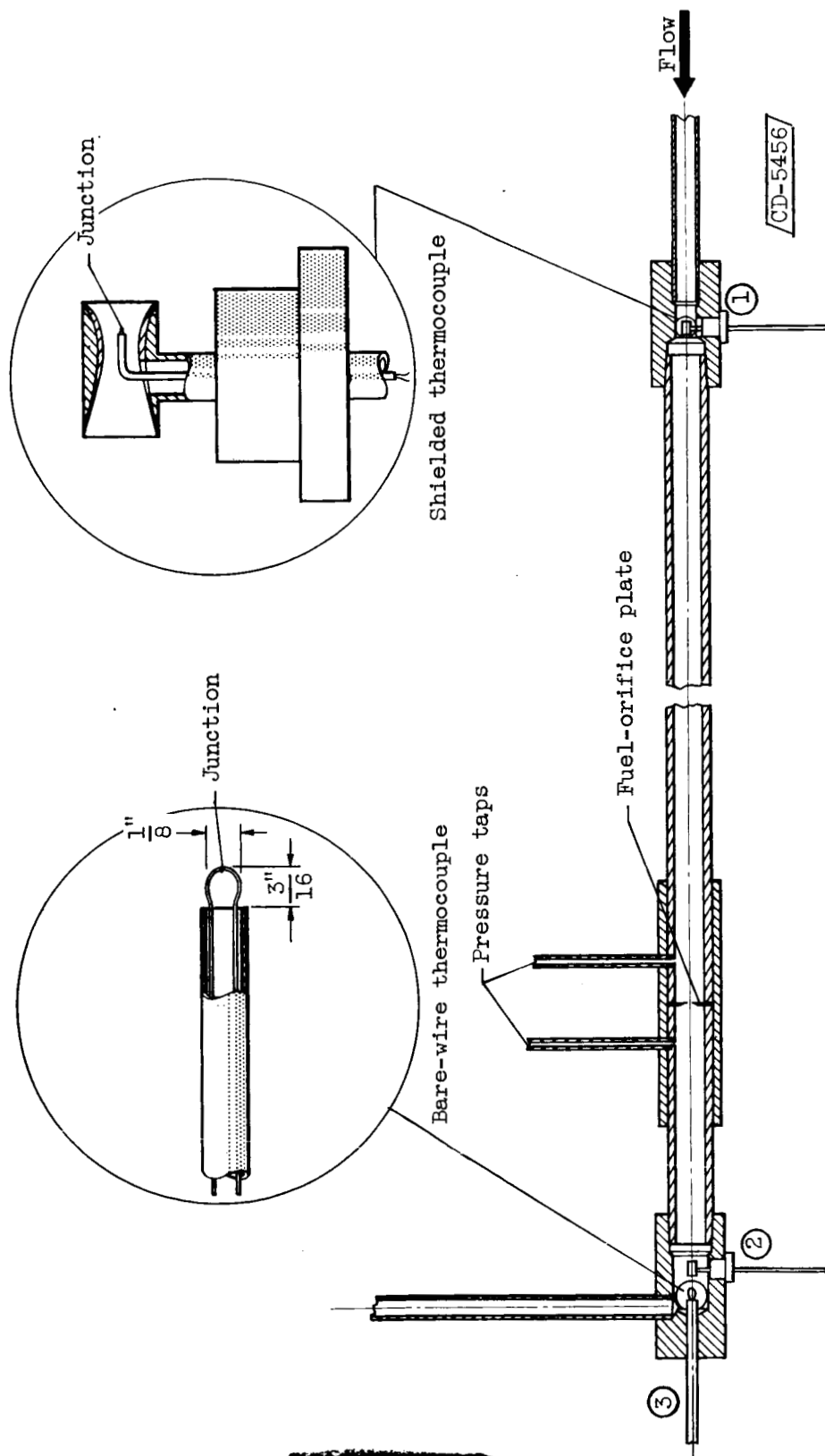


Figure 9. - Construction details of fuel orifice and copper-constantan thermocouples.

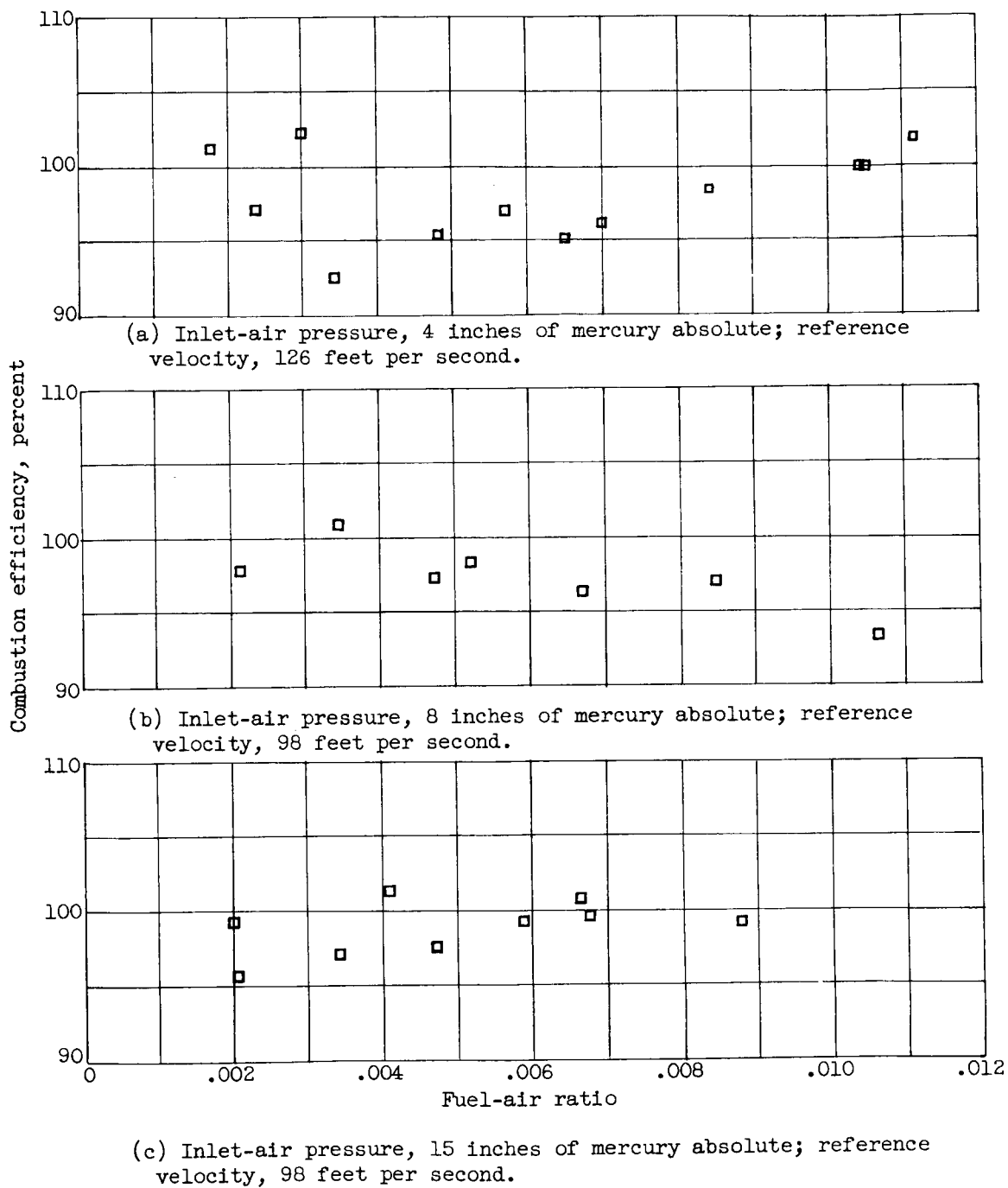
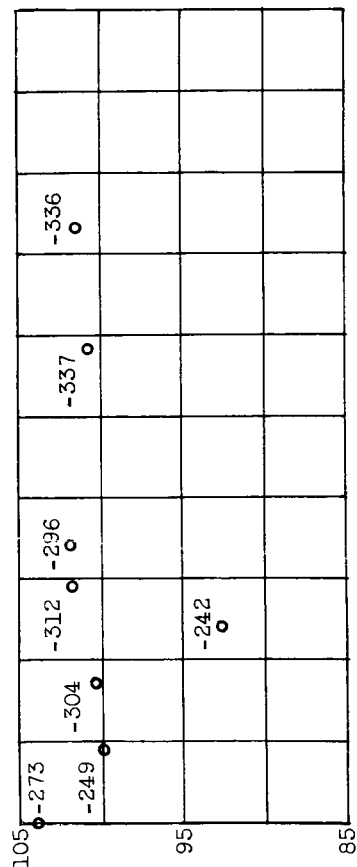
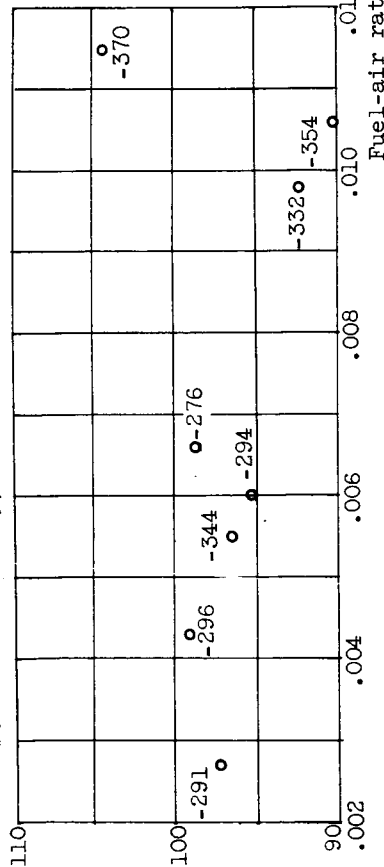


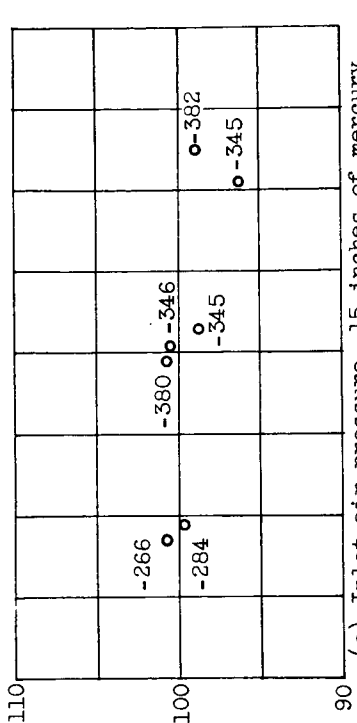
Figure 10. - Combustion efficiencies of J33 combustor with hydrogen fuel.
Fuel temperature, approximately 80° F; inlet-air temperature, 300° F.



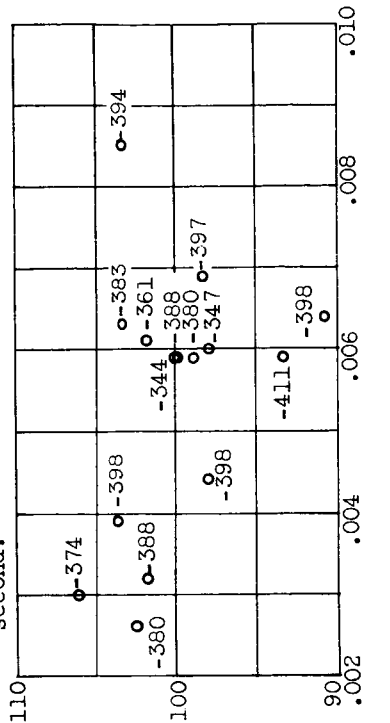
(a) Inlet-air pressure, 4 inches of mercury absolute; reference velocity, 126 feet per second.



(b) Inlet-air pressure, 8 inches of mercury absolute; reference velocity, 98 feet per second.



(c) Inlet-air pressure, 15 inches of mercury absolute; reference velocity, 98 feet per second.



(d) Inlet-air pressure, 30 inches of mercury absolute; reference velocity, 101 feet per second.

Figure 11. - Combustion efficiencies of J33 combustor with hydrogen fuel. Inlet-air temperature, 300° F; fuel temperature indicated at each data point.

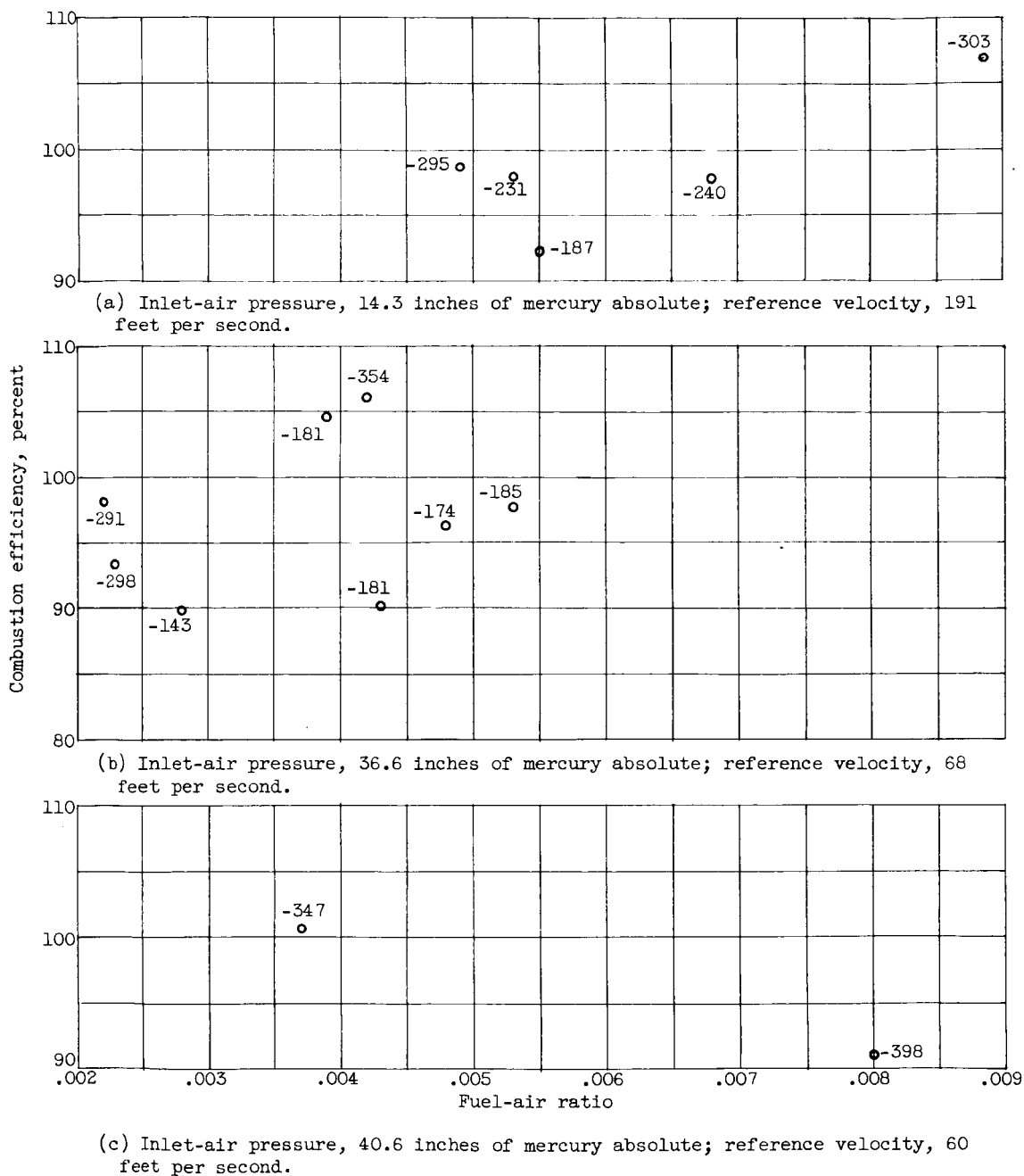


Figure 12. - Combustion efficiencies of vaporizer-tube combustor with hydrogen fuel. Inlet-air temperature, 300° F; fuel temperature indicated at each data point.

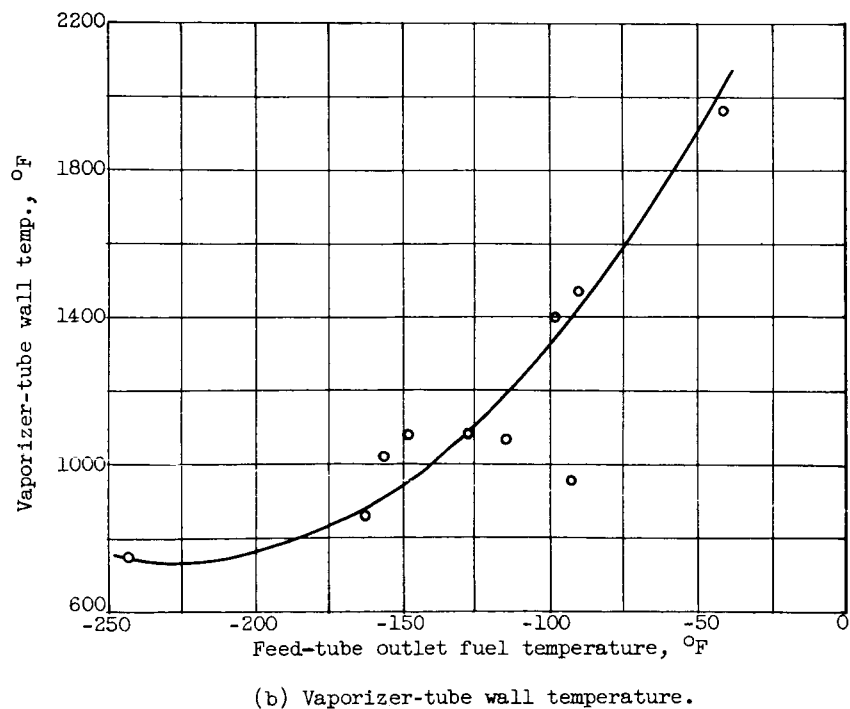
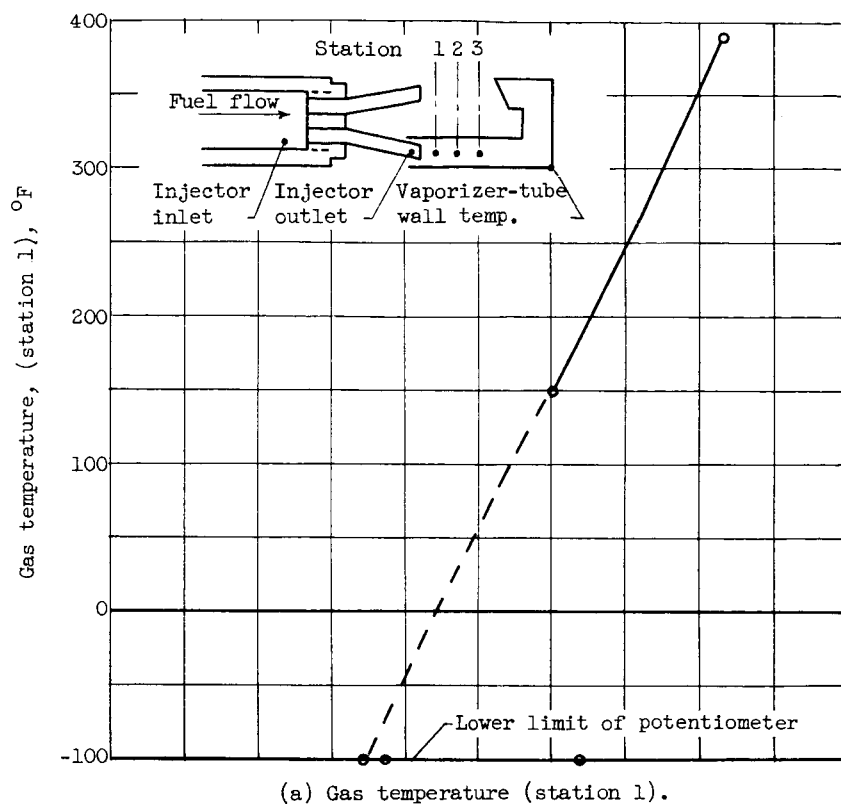
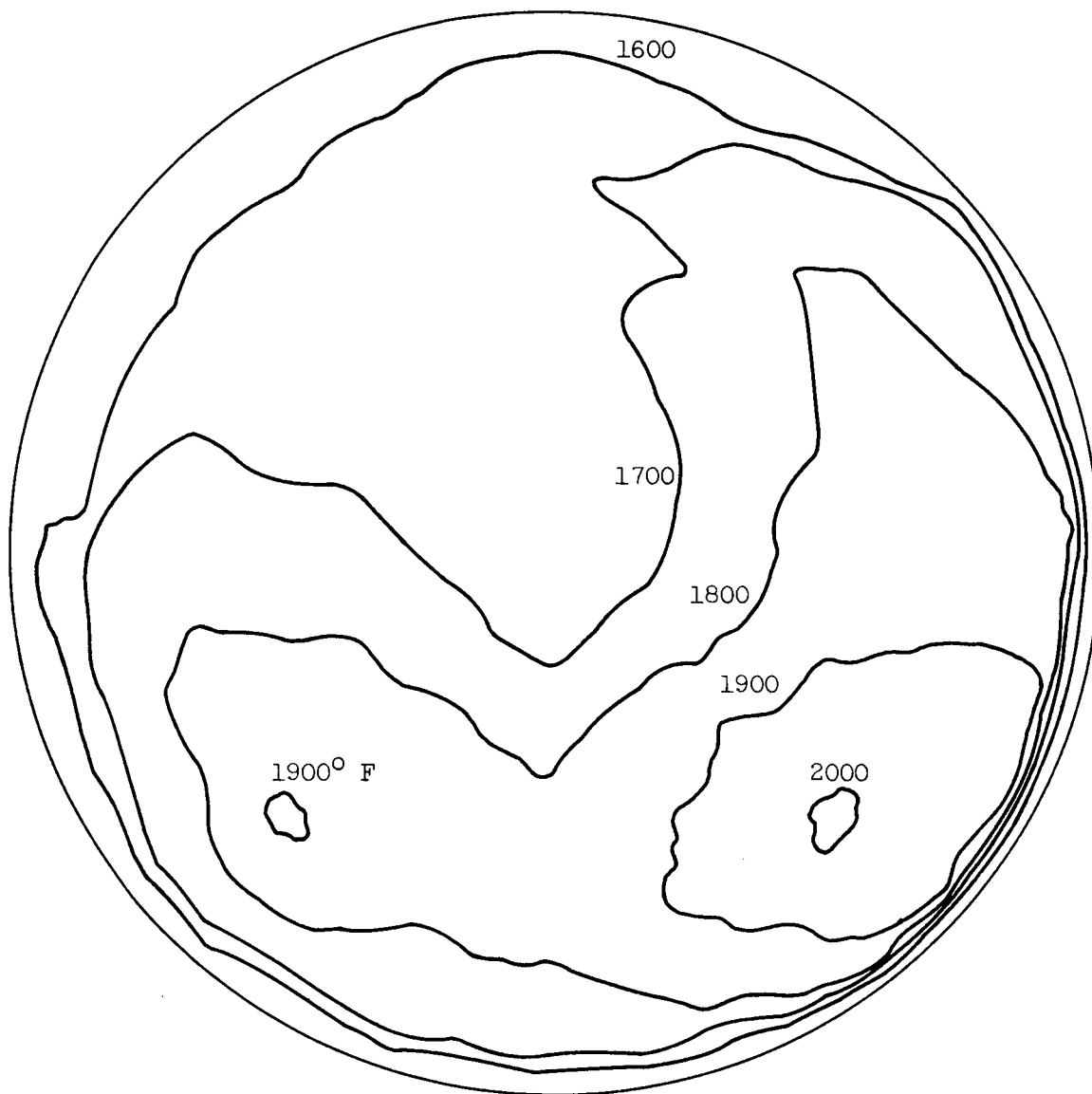


Figure 13. - Variation of gas and wall temperature with feed-tube outlet fuel temperature for vaporizer-tube combustor using cold hydrogen fuel.

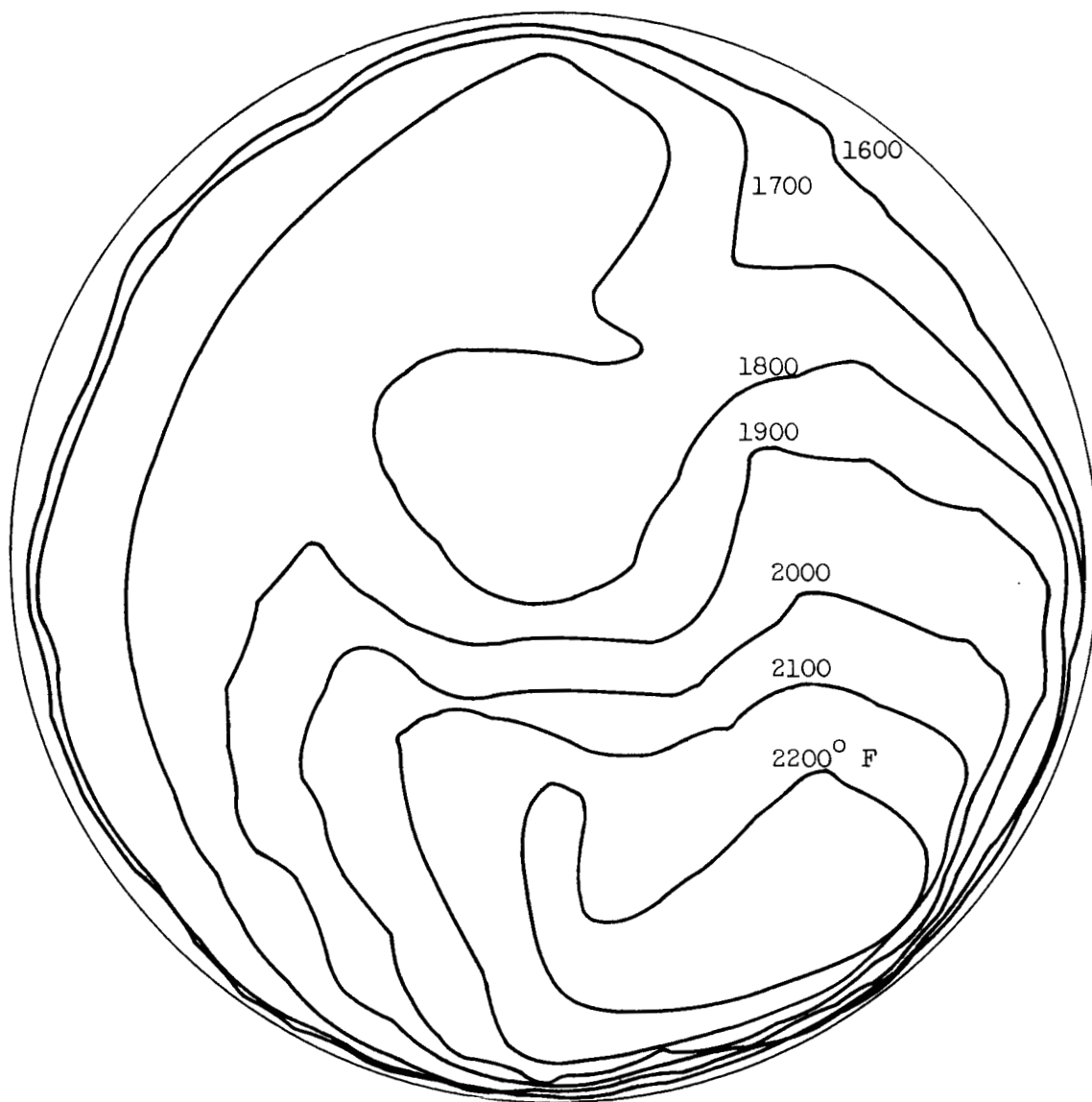


(a) Fuel temperature, 80° F; average outlet temperature, 1785° F.

Figure 14. - Exhaust-gas temperature pattern in J33 combustor. Combustor inlet-air temperature, 300° F; inlet-air pressure, 8 inches of mercury absolute; reference velocity, 98 feet per second.

4167

CR-5



(b) Fuel temperature, -370°F ; average outlet temperature, 1931°F .

Figure 14. - Concluded. Exhaust-gas temperature pattern in J33 combustor. Combustor inlet-air temperature, 300°F ; inlet-air pressure, 8 inches of mercury absolute; reference velocity, 98 feet per second.

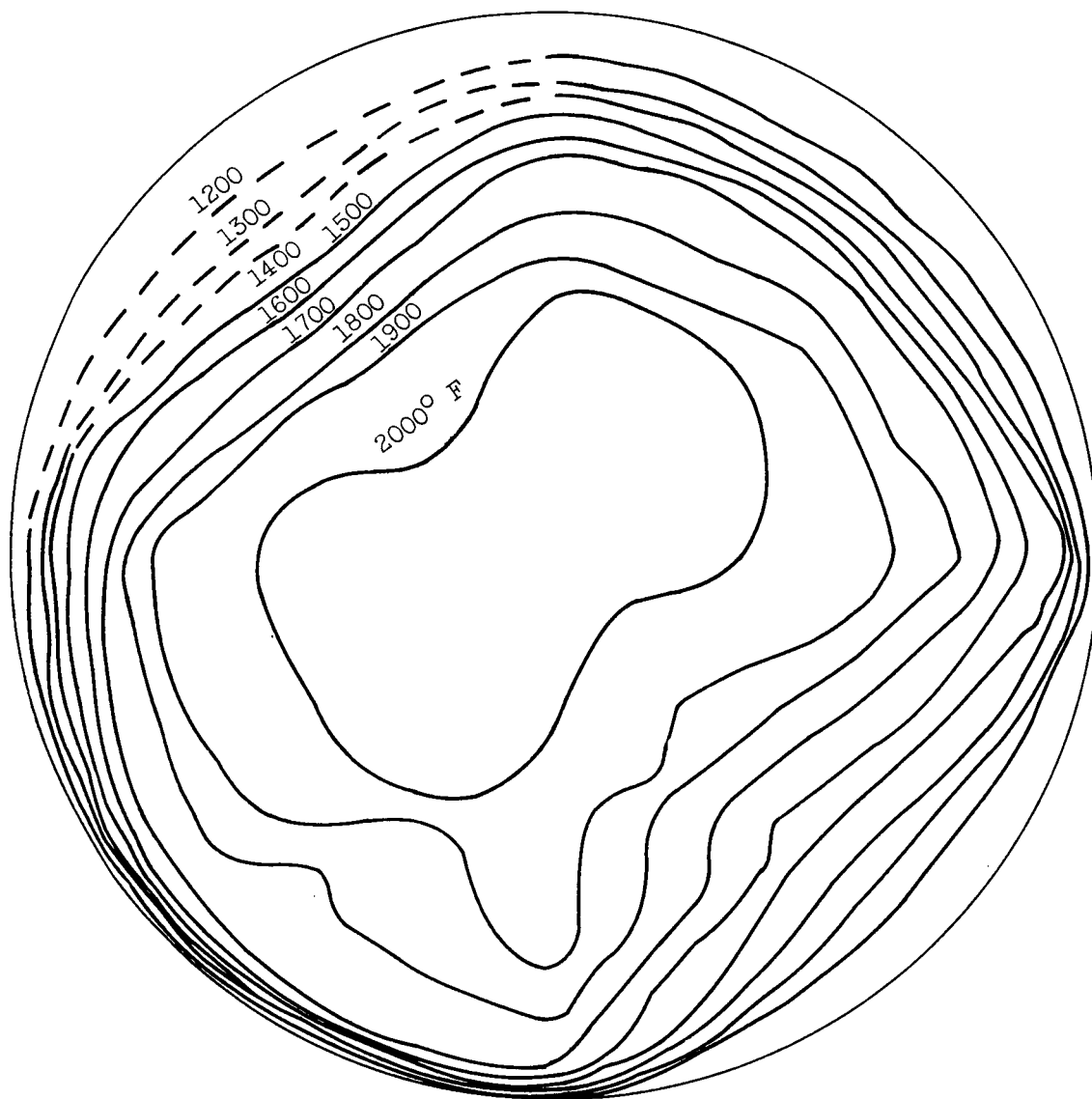
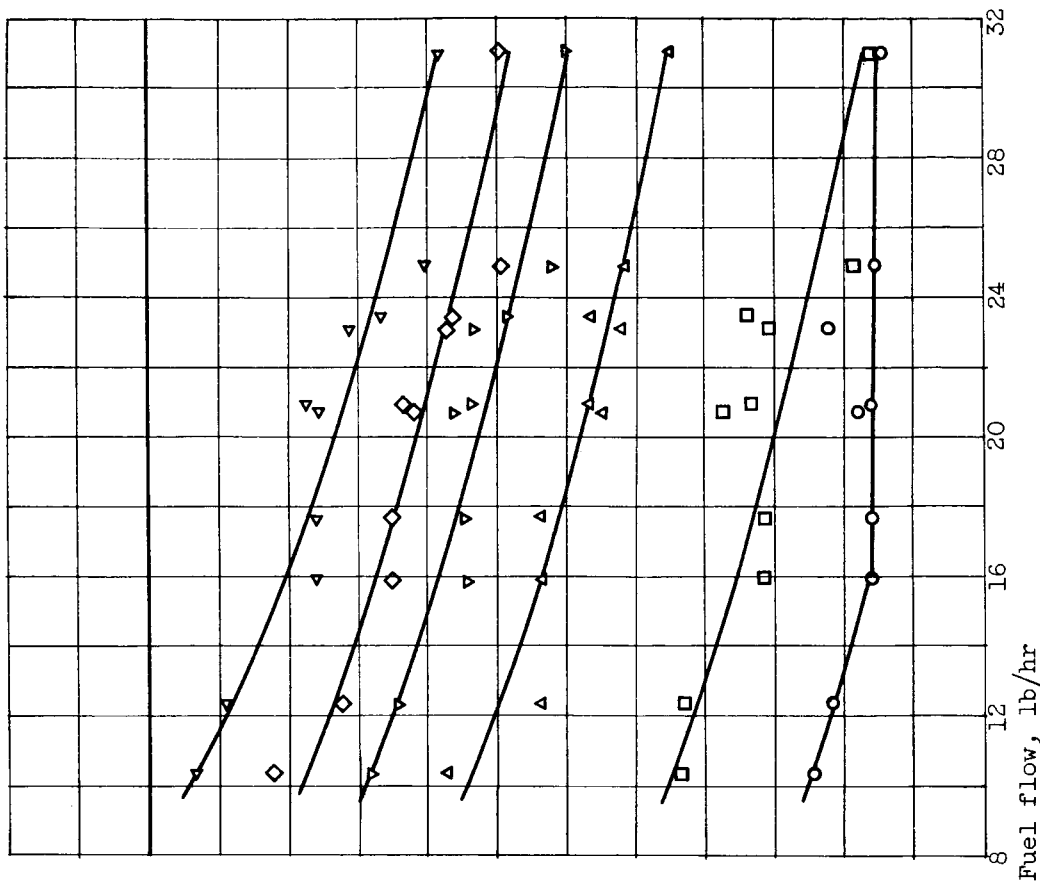


Figure 15. - Temperature pattern at outlet of vaporizer-tube combustor. Combustor inlet-air pressure, 15 inches of mercury absolute; inlet-air temperature, 300° F; reference velocity, 60 feet per second; fuel temperature, -303° F; average outlet temperature, 1748° F.

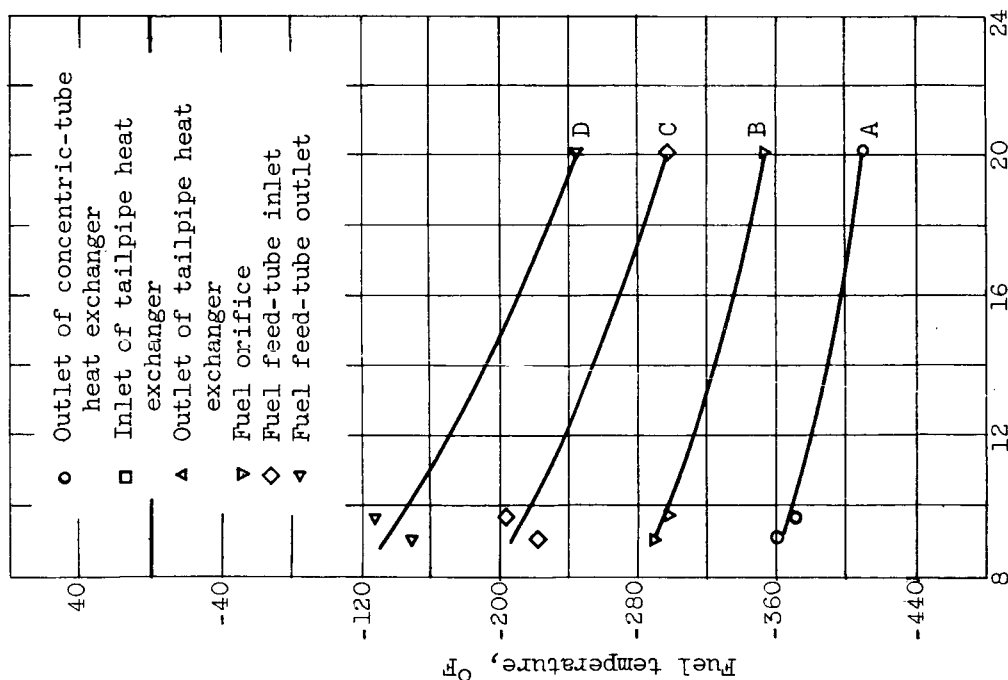
SECRET

4167

CR-5 back



(a) No flow in tailpipe heat exchanger.



(b) With flow in tailpipe heat exchanger.

Figure 16. - Fuel temperature at various stations in liquid-hydrogen fuel system.

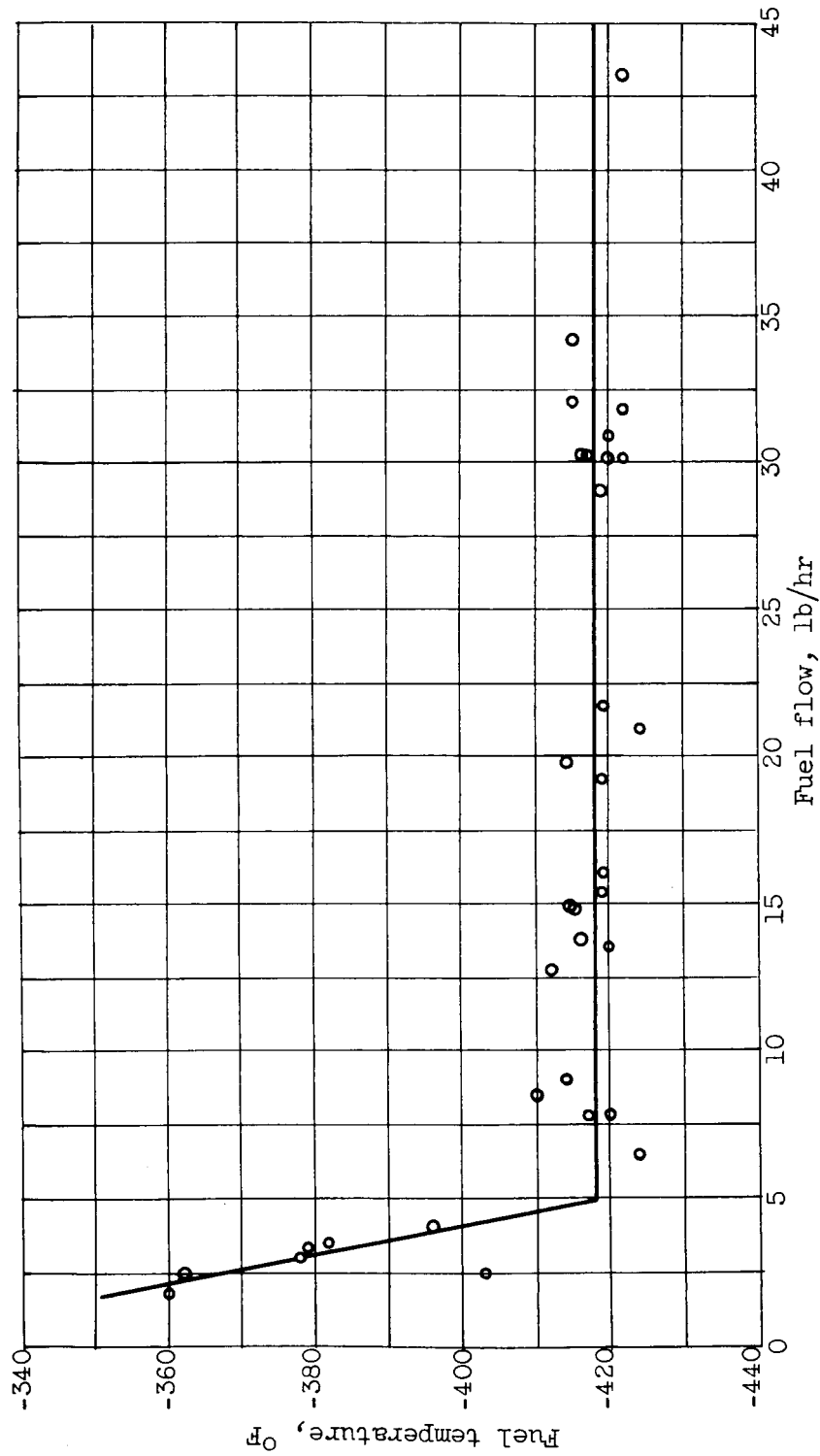


Figure 17. - Variation of fuel temperature with flow rate at inlet of concentric-tube heat exchanger.

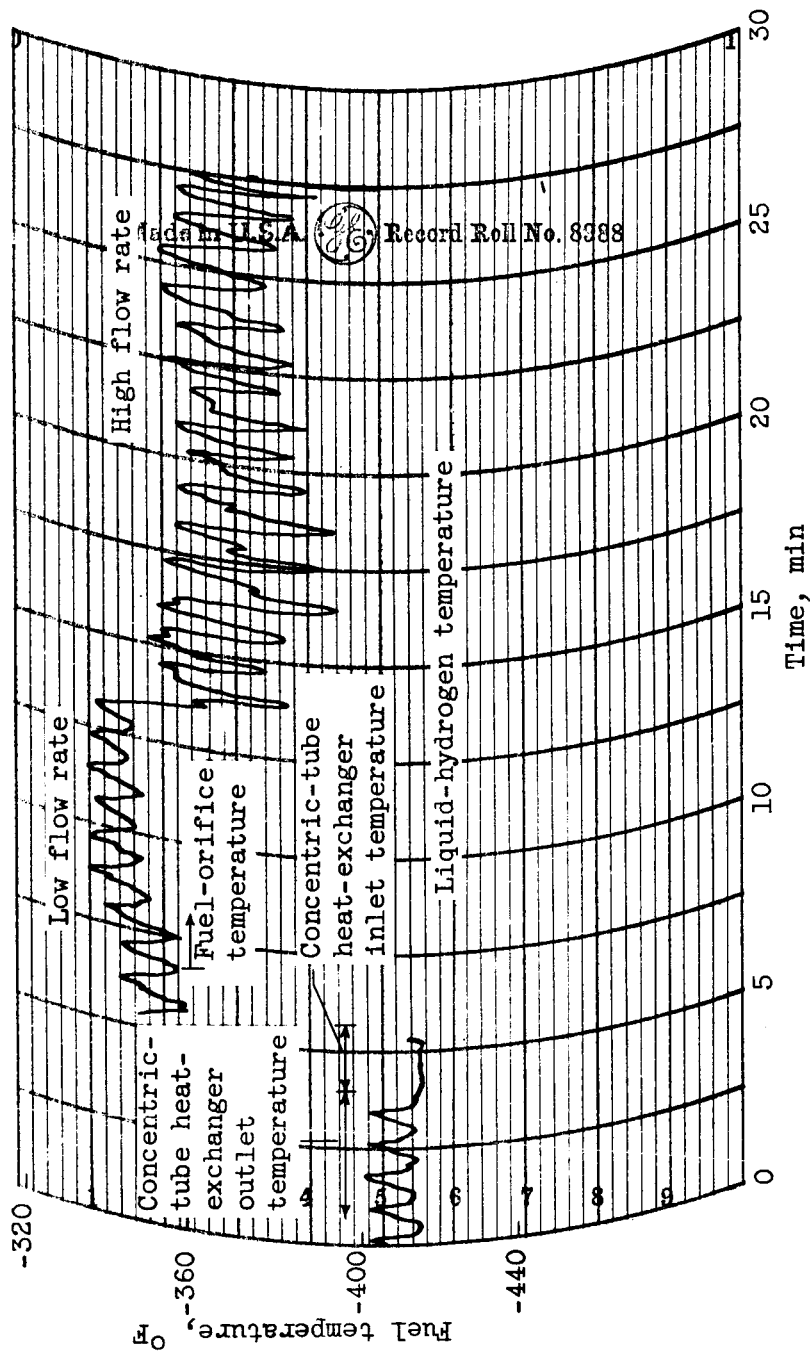


Figure 18. - Temperature oscillation in fuel line.

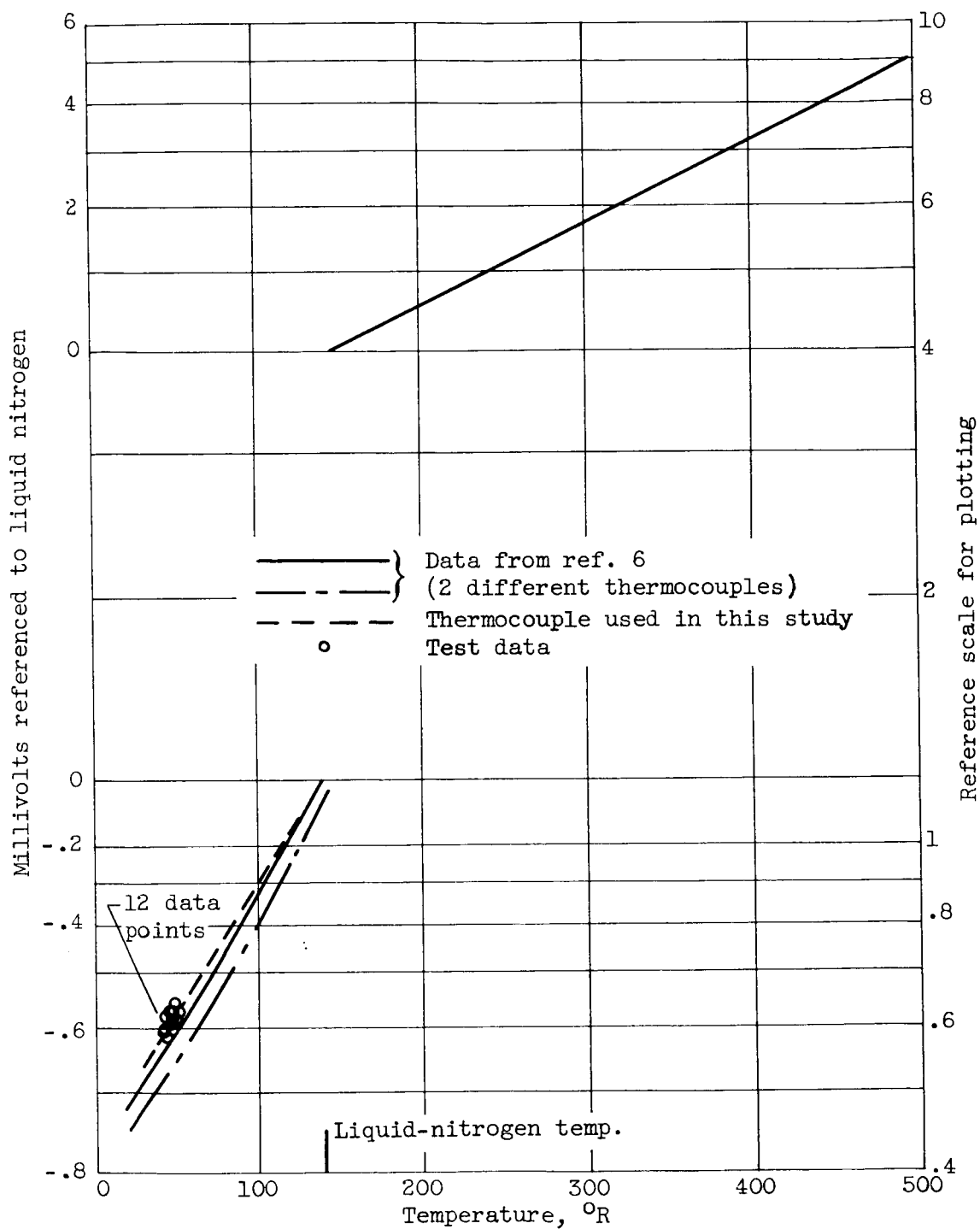


Figure 19. - Method of calibrating copper-constantan thermocouples used in investigation.

RECEIVED

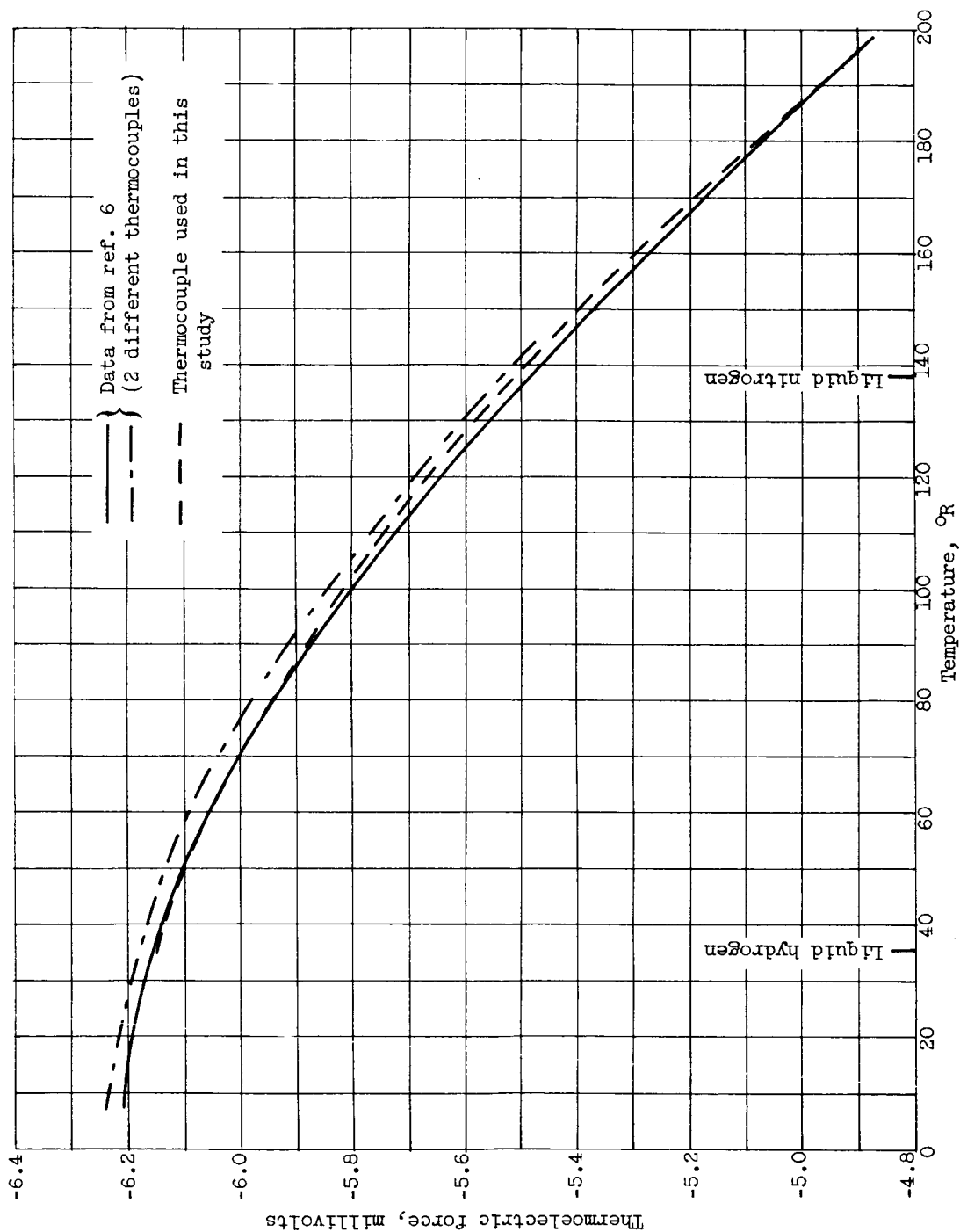


Figure 20. - Variation of millivolt output from three different copper-constantan thermocouples. Reference temperature, 32° F.

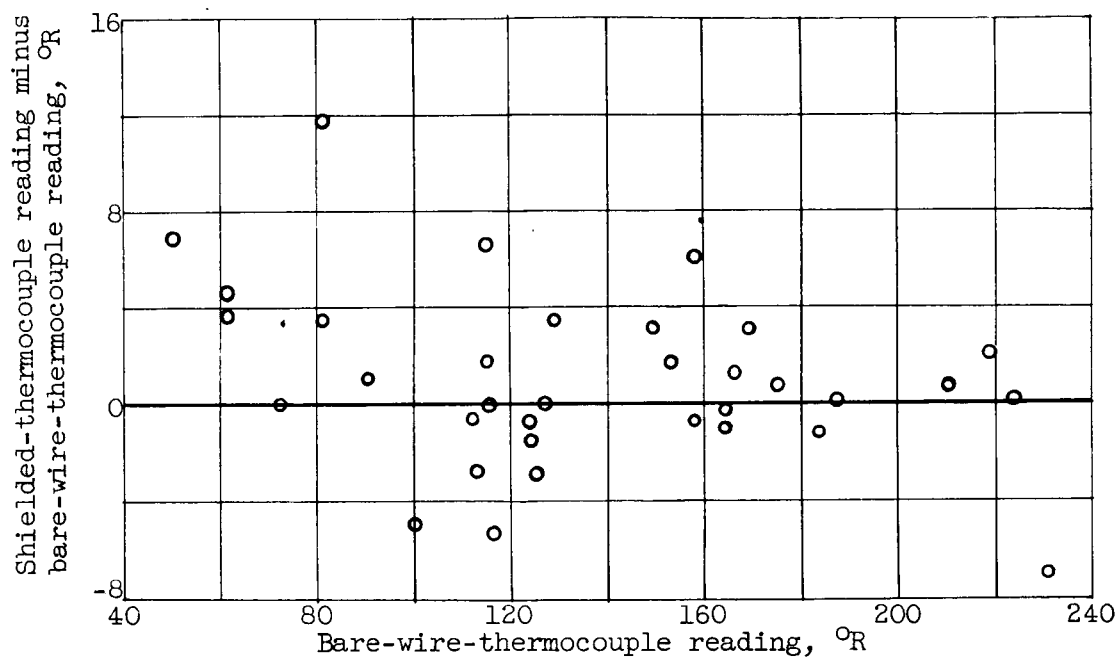


Figure 21. - Difference in temperature readings obtained with shielded and unshielded copper-constantan thermocouples.

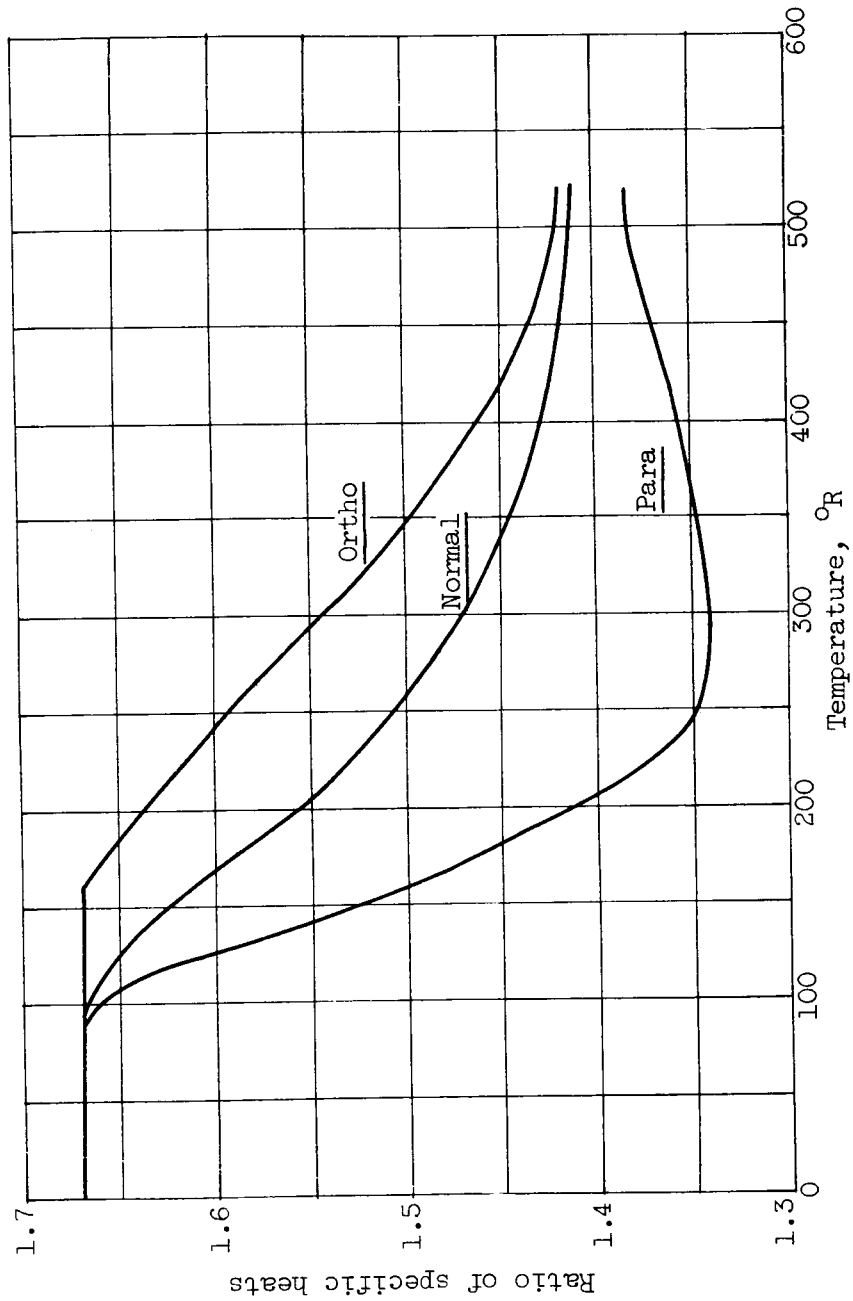


Figure 22. - Ratio of specific heats of hydrogen (ref. 7).